1-1-2008

Mass Spectrometry of Dendrimer Metal Complexes

Jason David Batchelor

MASS SPECTROMETRY OF DENDRIMER METAL COMPLEXES

Thesis submitted to
the Graduate College of
Marshall University

In partial fulfillment of
the requirement for the degree of
Master of Science in Chemistry

by

Jason David Batchelor

William Price, Ph.D., Committee Chairperson
Michael Castellani, Ph.D.
Leslie Frost, Ph.D.

Marshall University

May 2008

ABSTRACT

Mass Spectrometry of Dendrimer Metal Complexes

by Jason David Batchelor

Dendrimers are hyper-branched macromolecules with unique properties. They form using a "cascade-like" synthesis involving repetitive reaction steps. These steps are controlled, resulting in monodisperse dendrimers. Synthesis is divergent, core to exterior, or convergent, exterior to core. Dendrimers are created from various molecules with numerous functional properties. They are used as catalysts, diagnostic agents, and others.

This thesis studies 1st generation poly(propylene) imine, consisting of a diaminobutane core with 4 propyl amine branches. Fragmentation of protonated and metal (Co, Ni, Cu and Zn) complexed dendrimers was analyzed by ion-trap mass spectrometry. Two isotopically labeled dendrimers were synthesized for neutral loss identification and possible fragmentation mechanisms.

Protonated dendrimer fragments through substitution mechanisms. Similar fragments are identified in metal complexes, but the dendrimer is coordinated in a specific geometry with the metal and elimination mechanisms dominate. Fragmentation schemes for all complexes are presented. Neutral mass losses are compared and unique fragments discussed.

DEDICATION

This thesis is dedicated to my wife. Without her love, I would have never become the man I am today.

I would also like to thank my mom and brother who have always tried to keep me on the right path, and to my dad, for the analytical mind he passed on to me.

To all my other family members, I thank you all. I am truly blessed to have each and every one of you in my life.

ACKNOWLEDGEMENTS

I would like to acknowledge my advisor, Dr. Price, for his insight and instruction during my tenure at Marshall.

I would also like to thank the entire Chemistry department for their instruction and help during my three years in Huntington. I learned a great deal from each of you.

TABLE OF CONTENTS

LIST OF FIGURES

CHAPTER ONE

CHAPTER THREE

CHAPTER FOUR

LIST OF TABLES

CHAPTER FOUR

CHAPTER ONE: INTRODUCTION

Dendrimers, from the greek *dendra* meaning "tree," are hyper-branched macromolecules with unique properties. Although the concept of branching networks can be traced to the 1940's and the infinite network theory of Flory and Stockmayer,[1] the first synthetic approach wasn't documented until the late 1970's when Fritz Vögtle, at the University of Bonn in Germany, began creating these tree-like structures.

Vögtle utilized a repeating-step principle to generate these acyclic, branched molecules.[2] This "cascade-like" synthesis involved a Michael addition of acrylonitrile to a mono-amine followed by reduction of the nitrile groups to the primary amine using the homogenous catalyst Cobalt(II)/$NaBH_4$.[2] The synthesis, however, was complicated by low reduction yields and difficult purification that limited the number of reaction cycles. In the early 1990's, large scale synthesis of an amine-based dendrimer was achieved by Mülhaupt,[3] and de Brabander-van den Berg[4] utilizing Raney-Ni or -Co, respectively, with $H_{2(g)}$ as a heterogeneous catalyst to reduce the nitrile functionalities.

Donald Tomalia, concurrent with Vögtle, and working at Dow Chemical, used methyl acrylate added to various amines and subsequent reaction with α,ω-diaminoalkanes to create "cascade" molecules.[5] Several research groups have also synthesized dendrimer-type molecules using other reactants. Denkewalter used the amino acid lysine to create a branching molecule possessing unsymmetrical branch lengths.[6] Newkome has reported synthesis of a symmetrical branched macromolecule termed an "arborol," that contains three cascade spheres attached to a benzene core.[7] In general, these reactions involve the molecule "growing" from a central point toward the outside; this is called the *divergent* synthesis. However in 1990, Fréchet introduced an alternate synthetic approach to creating these types of molecules that "grows" the dendrimer

from the outside to the core; this is called the *convergent* synthesis.[8] These two synthetic routes will be discussed in more detail later in this introduction.

Dendrimers have three defining regions: (i) initiator **core**, (ii) branching **interior** and (iii) functional **exterior** (Figure 1.1).

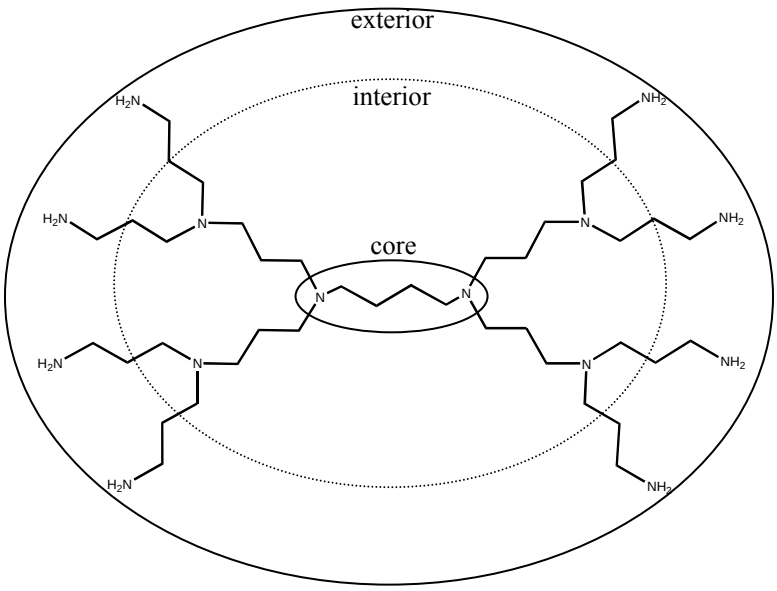

Figure 1. 1 2nd generation poly(propylene) imine dendrimer illustrating core, interior and exterior "shells."

The initiator core has functional units that can react with the monomer. The core multiplicity (N_c) is defined as the number of branching sites on the core (e.g. N_c for 1,4-diaminobutane = 4). The core is the fundamental unit that anchors the monomer branches (dendrons). The size, shape, multiplicity and specialized function of the core will greatly influence the dendrimer. Researchers have synthesized dendrimers with cores consisting of chromophores, chelating groups, metals and others.[1]

The interior is created by the monomers attached to the core and successive monomer functional sites. Each monomer has branching sites (branching multiplicity (N_b) ≥ 2) that can be reacted in a step-wise manner with additional monomers to increase the size of the dendrimer. Each successive set of reactions leads to a new "generation" of dendrimer. The reaction set

varies according to the dendrimer and can be complicated as protection/deprotection strategies may need to be used. The type of monomer defines the overall topology of the dendrimer.

The exterior of the dendrimer has terminal groups that can be modified. Functionalization of the dendrimer exterior leads to dendrimers possessing varying properties. Because the number of terminal groups (z) increases exponentially with linear increase in generation ($z = N_c N_b^G$ where G is the generation number), the number of generations is limited.[1] This limit, known as the "starburst limit," is due to congestion at the branching surface that reduces the ability to create a monodisperse dendrimer. The type and multiplicities of core and branching units influence this limit; the higher the multiplicity and the shorter the branching units, the faster the limit is reached.

Two synthetic routes are used to create dendrimers: divergent and convergent. The divergent approach begins at the initiator core and works outwards toward the periphery using a set of reactions (Figure 1.2). Each set leads to a new generation of dendrimer and a concomitant increase in the molar mass of the molecule. To minimize structural defects, it is important that each reaction set is completed before a new set begins. Using efficient, high-yield reactions, it is possible to synthesize a 10th generation dendrimer with 3000 end groups and a molecular weight

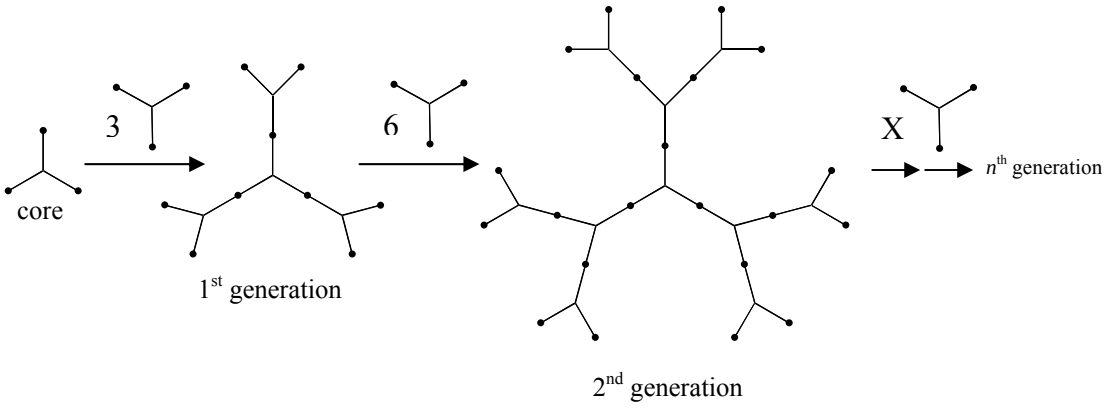

Figure 1. 2 Schematic representation of a divergent synthesis of a dendrimer with $N_c = 3$ and $N_b = 2$.

around 700,000.[9] However, with each generation the number of reaction monomer units increases exponentially, leading to the possibility of incomplete addition and a polydisperse dendrimer. This polydispersity, that occurs as the dendrimer approaches its' starburst limit, is often difficult to detect as the incomplete dendrimers differ by only a few monomers.

The convergent method, first proposed by Fréchet and Hawker,[8] is simply the reverse of the divergent method; synthesis begins at what will be the exterior and works its way toward the core. Dendritic "wedges" are formed and in the final reaction step the desired number of wedges is added to a multifunctional core (Figure 1.3). As opposed to the divergent method, the number

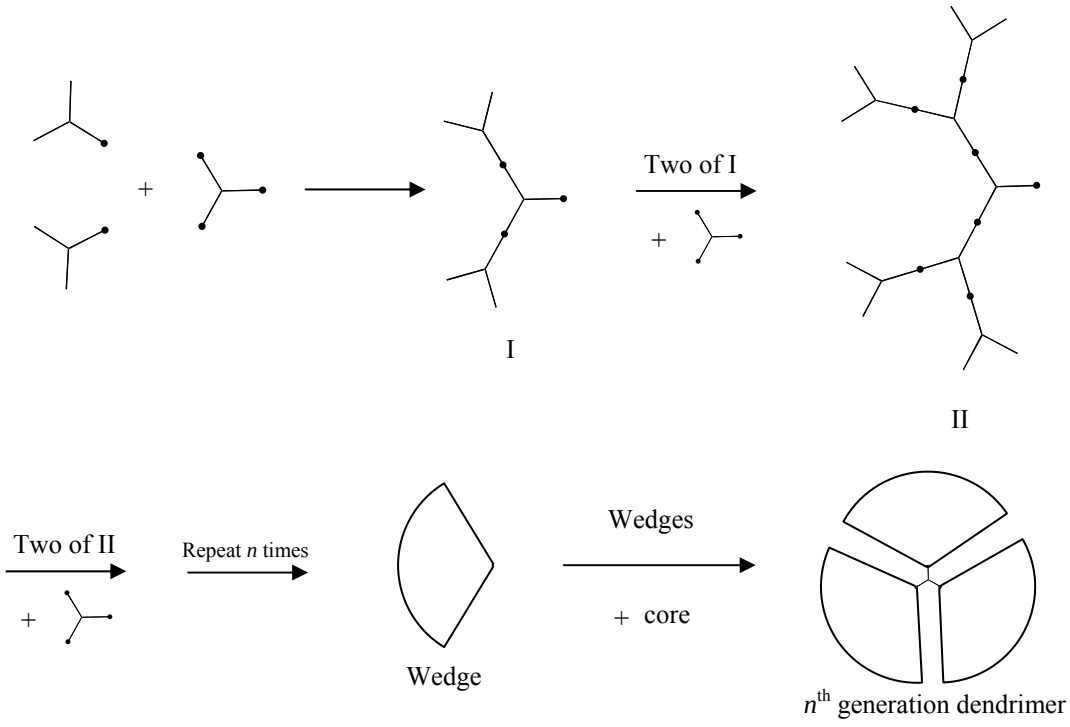

Figure 1. 3 Schematic representation of the convergent synthesis of a dendrimer with $N_c = 3$ and $N_b = 2$.

of reacting units in each step of the synthesis is small; two large units react with a smaller multi-functional unit. In addition, large excesses of reagent can be avoided without sacrificing high yield. As a result, the reactions no longer need to be as efficient, leading to different reaction

types and more monomers available for use. The versatility of the convergent method is seen in the ability to create segment-block dendrimers that involve adding wedges of differing chemistry to a common core.[9] The total number of reaction steps is not reduced when compared to the divergent method and the higher generation wedges often experience steric problems in the final attachment to the core molecule. Thus, the convergent method has not been as widely used to create new types of dendrimers.

The unique structure of dendrimers gives them features that provide advantages over their linear analogs. Linear polymers exist in solution as loose, random coils; dendrimers, as branch density increases, undergo a reorganization and take on a ball-like form.[10] For example, the 9th generation poly(amidoamine) dendrimer (PAMAM) has 3069 monomer units, a molecular weight of 349,883 g/mol, and a diameter of 98 to 105 Å.[11] This packed ball structure creates void space in the interior of the dendrimer. This void space combined with the functional exterior is the basis for many dendrimer applications.

One area where dendrimers are showing promise is catalysis. Classic linear polymers have been made into functional polymers, ones that have reactive functional groups that can participate in chemical processes without degradation of the original polymer chains.[12] Of the two types of catalysts, homogenous and heterogeneous, the former is the more selective due to its solubility in the medium in which it acts, typical small size, and well-defined structure.[10] Yet it is difficult to isolate and reuse like a heterogeneous catalyst. The ideal catalyst should be soluble (homogenous), multifunctional, adopt a configuration where every active site is available to migrating reactants, unlikely to be inhibited by catalytically inactive species, recoverable and reusable.[13] Dendrimers, with their large surface area to volume ratio (as much as 1000 m^2/g)[11] capable of housing multiple catalytic sites, can combine the benefits of a homogenous catalyst

(faster kinetics, accessibility of the catalytic site) with the simple separation and reuse of a heterogeneous one.[13,14]

Reetz and coworkers have functionalized 2nd and 3rd generation PPI dendrimers with a double phosphinomethylation at the periphery and complexed those groups with palladium metal ions.[6] The functionalized dendrimers, used as catalysts in the Heck reaction, were found to have significantly higher catalytic activity than their monomeric analogs. Suslick et al. have used the convergent method to attach 4 dendrons with *tert*-butyl terminal groups to a metallo-porphyrin core to study regioselective catalysis in the epoxidation of olefins.[6] The dendrimers showed greater selectivity to linear alkenes over cyclic ones in a mixture. This is attributed to steric hindrance at the periphery and greater accessibility of linear molecules to the catalytic center. Crooks at Texas A&M University has created dendrimer-encapsulated metal nanoparticles using poly(propylene) imine (PPI) and poly(amidoamine) (PAMAM) dendrimers complexed with various metals (gold, platinum and palladium) and has studied their catalytic properties, such as hydrogenation of alkenes.[15,16]

Dendrimers are becoming more and more useful in the fields of biochemistry and medicine due to their unique properties; two areas of interest are micelle/liposome mimicry and targeted drug delivery. A micelle system contains self-assembling amphiphilic molecules that, in solution at the proper concentration, form a solvent incompatible inner core and a solvent compatible outer shell. Due to the properties of dendrimers, the surface units can be functionalized to have a different polarity than the interior. Because of their packed-ball structure these amphiphilic dendrimers can be viewed as "covalently fixed microdomains, which mimic either regular or inverse micelles, depending on the compatibility of the dendrimer surface with water.[1]" Building a micelle mimic this way lets the head group multiplicity be determined

by the synthesis of the dendrimer (i.e. generation number) instead of self-formation based upon thermodynamic and entropic effects. For instance, Meijer and co-workers have functionalized multiple generations of PPI dendrimers with variety of long-chain alkanes to create an inverted micelle mimic that has a nonpolar periphery and a polar interior.[17]

Liposomes are small bi-layer vesicles in a cell which are used for storage and transport. They differ from micelles in that they have a bi-layer membrane with an aqueous interior; micelles have a single layer with no internal solvent. Because of the packed ball structure of dendrimers, there are internal void spaces that can be used to "house" molecules of interest. Molecules can either be covalently linked to the interior of the dendrimer during synthesis and then the remainder of the synthesis occurs encapsulating the guest molecules[18] or non-covalently associated with the dendrimer depending on the properties of the dendrimer interior and the guest molecule (i.e. a polar dendrimer interior provides non-covalent binding sites for a polar guest). In a molecular dynamics simulation, a 6^{th} generation PAMAM dendrimer was shown to host 10-20 dopamine molecules in the internal void space through hydrogen bonding between the dendrimer interior and the amine and hydroxyl functionalities of the dopamine.[1]

This micelle/liposome mimicry has led to dendrimers being used for drug delivery. One method is to synthesize a dendrimer with surface units that are water-soluble, bio-degradable, and inner shells containing an appropriate amount of drug so as the dendrimer is degraded, a uniform supply of drug is released.[9]

Another widely researched method is to use a properly functionalized dendrimer to be the so-called drug. Roy et al. have linked eight sialinic acid units to a multi-branched L-lysine dendrimer and preliminary tests with influenza A virus have indicated that the dendrimer is a strong inhibitor of human erythrocyte hemagglutination, reducing the risk of infection.[19] In

addition, cell surface carbohydrates are involved in various aspects of cellular function (e.g. growth, regulation, inflammation and the infection process), so well-defined glycodendrimers could find use as therapeutic agents in the prevention of viral and bacterial infections.[19] For instance, Starpharma has recently completed Phase I clinical trials on a dendrimer based drug called VivaGel. This 4th generation poly-lysine dendrimer with naphthalene disulfonate terminal groups prevents HIV infection by binding to the gp120 glycoprotein receptor on the virus' surface. This prevents the HIV from attaching to the bodys' T-cells, its intended target.[20]

Dendrimers are also finding use as advanced diagnostic agents. When a person comes to the emergency room with chest pains, it may or may not be a true heart attack. The faster the correct diagnosis, the better off the patient is, especially in the case of a true heart attack. Singh with Dade Behring is working on an instrument that detects certain blood biomarkers that are released as a result of heart muscle damage. The instrument analyzer uses a 5th generation PAMAM dendrimer with covalently bound antibodies specific for those biomarkers.[20]

Within the body, small molecule MRI agents use metal ions for contrast. Because dendrimers can encapsulate or chelate multiple metal ions in a relatively small area, more detailed images can be obtained. In addition, the dendrimers are larger than the typical small molecule agents so, if given intravenously, the dendrimer agent tends not to leak from the bloodstream, giving clearer images.[11,20]

Dendrimers have also found use in the fields of nanoelectronics and materials science. Tomalia's group has synthesized a hollow rod-shaped dendrimer that is around 50 Å in diameter and 3000-4000 Å in length. This could be used as a molecular wire given the correct functionality.[11] The high aspect ratio is similar to that of carbon nanotubes. Miller at the University of Minnesota is working with PAMAM dendrimers functionalized with electron-

donating imide groups in an effort to make a three-dimensional conducting polymer. This polymer may have unique properties similar to fullerenes that can conduct electricity without resistance at a higher temperature than that of any other molecular conductor.[10]

In the realm of materials science, the first thermotropic liquid crystalline dendrimer based on ether linkages was created by Percec and Kawasumu. The flexibility of the dendrimer allows the molecule to transition between the solid and liquid crystalline state between 20 and 50 °C.[18] Fréchet at Cornell is working with non-homogenous mixtures of dendrimers added to traditional polymers of similar composition to produce coatings of extraordinary strength and durability.[11] Polyscience, based in Pennsylvania, sells sizing kits that consist of starburst dendrimers labeled with a different fluorescent tag for each size.[11] Tomalia's group is working on making thin films of cross-linked dendrimers to be used as membranes for separating various gases and biological molecules, because the size of the pores between the dendrimers varies according to generation and composition.[11]

Dendrimer applications are widely varied and more dendrimers with different applications are being created every day. Dendrimer catalysts are one of the more promising applications. As mentioned previously, metal-dendrimer complexes have been shown to have solution-phase catalytic properties.[6,15,16] Characterization of these dendrimers and their properties has generally been accomplished with solution-phase characterization tools like nuclear magnetic resonance (NMR), optical spectroscopy and surface characterization tools like electron and atomic force microscopy. It is entirely possible that these types of complexes could also have similar gas-phase properties. In order to investigate these properties, the analytical technique of mass spectrometry was used.

Mass spectrometry is a technique that separates and detects gas-phase molecules according to their mass-to-charge ratio. Ionization of the complexes was achieved using electrospray ionization. This ionization source uses an infusion of an analyte solution through a nebulizer, producing a spray of droplets. A voltage potential is applied between the nebulizer needle and a heated capillary. A stream of dry nitrogen and the heated capillary effectively desolvate the droplets, leaving charged analyte molecules in the gas-phase. These molecules are guided into the ion-trap, where they undergo stabilizing collisions with neutral helium atoms. The molecules are then activated and sequentially ejected and detected from low to high mass-to-charge ratio. In addition, a molecule of interest can be isolated in the ion-trap by ejecting all other molecules except the specified one. This molecule can then be activated by repeated collisions with the neutral helium atoms until the molecule builds up enough internal energy to dissociate and the molecule fragments. This is called collision-activated dissociation. The fragments are then sequentially ejected and detected.

This thesis focuses on the characterization of 1st generation poly(propylene) imine dendrimer, both protonated and metal-complexed. Four divalent metals were used; cobalt, copper, nickel and zinc. Fragmentation of the protonated and metal-complexed dendrimers were analyzed and compared in an effort to gain knowledge about how these complexes behave in the gas-phase; only then, can one begin to study their possible gas-phase catalytic properties.

CHAPTER TWO: EXPERIMENTAL

MATERIALS

1st generation PPI dendrimer, 1,4 diaminobutane and acrylonitrile-2-d were purchased from Aldrich Chemical Company. Acrylonitrile-^{15}N was purchased from Isotec. Zinc(II), Cobalt(II), Nickel(II), Copper(II) acetates and acetonitrile were purchased from Fisher Scientific. All reagents were used without further purification.

MASS SPECTROMETRY

Complexes were formed in solution by mixing 2 mM aqueous PPI dendrimer solutions with 10 mM aqueous solutions of metal(II) acetate. Mixed solutions were diluted 1:1 with acetonitrile and electrosprayed into a Thermo Finnigan LCQ quadrupole ion-trap mass spectrometer at a flow rate of 3 μL/min and a source potential of 4.1 kV. Gas-phase complexes were isolated and activated by collisions with He buffer gas. Complexes and collision fragments were identified and tabulated based on charge state, collision energy and complex partner.

MODELING

The thermochemistry of proposed fragmentation mechanisms was calculated using the BMK/6-311+G** model chemistry. Vibrational frequencies were calculated at the B3LYP/6-31G* level.

The relative standard Gibbs free energy ($\Delta\Delta G^{\circ}$) for the Zinc-PPI complexes was calculated at the B3LYP/6-31G* level. Four different conformations were compared.

SYNTHESIS

The synthesis of the isotopically labeled dendrimers was accomplished using the following method adapted from Meijer.[4] The full procedure is listed for the ^{15}N-labeled dendrimer. The major deviations to that procedure are listed for the ^{2}H-labeled dendrimer.

A. ^{15}N-labeled dendrimer

a. 0.0200g of diaminobutane was dissolved in 1 mL of water and placed into a small round bottom flask with a stir bar.
b. The vial of ^{15}N-labeled acrylonitrile (~100 mg) was added to the flask.
    i. Note: Upon addition of the acrylonitrile, the solution turned purple and then brown over time, presumably due to the hydroquinone used to stabilize the acrylonitrile
c. The solution stirred at room temperature for 45 minutes.
d. Two aliquots (about 1.5 mL each) of diethyl ether were added to the flask, stirred, and then all the solution was removed to a conical vial.
e. The solution was allowed to separate and the ether layer (containing the nitrile terminated dendrimer) was placed back into another small round bottom flask with a stir bar.
f. The ether was slowly evaporated off under vacuum. Gentle warming was necessary to remove ice crystals forming on the bottom of the flask.
g. After evaporation, the flask was placed under a stream of dry N_2.
h. 2 mL's of dry tetrahydrofuran was added to the flask, still under N_2, and allowed to stir for 5 minutes.
i. Approximately 0.10 g of lithium aluminum hydride was added to the flask.
    i. Note: A long stemmed glass funnel was used to add the LAH to prevent the powder from dispersing due to N_2 outflow.
j. The solution was allowed to react for 1 hour. A slightly warm water bath was used to gently heat the solution.
k. The unreacted LAH was quenched by slowly adding water dropwise, until a white precipitate formed and fell out of solution.
l. The solution was then extracted to a glass vial.
m. Approximately 100 μL of this solution was mixed with 1.5 mL of 50:50 Water:ACN before introduction into the mass spectrometer.

B. ^{2}H-labeled dendrimer

a. The diaminobutane was dissolved in 1 mL of D_2O to ensure complete addition of deuterium to the β-carbons.
b. Acrylonitrile-2-d was added to the flask. No color change was noted upon addition of the acrylonitrile.
- All remaining steps were unchanged.

CHAPTER THREE: 1st GENERATION PPI DENDRIMER

SYNTHESIS

Synthesis of the PPI dendrimer is done in a divergent manner and begins from a 1,4 diaminobutane core. The core undergoes a double Michael addition with acrylonitrile at each nitrogen. This results in a nitrile terminated 1st generation dendrimer. Reduction of the nitrile groups to their amine functionality is achieved with a heterogeneous catalyst such as Raney Co with $H_{2(g)}$, or a homogenous catalyst like lithium aluminum hydride (LAH). The heterogeneous catalyst is the preferred method of reduction in large scale synthesis due to the recovery of the catalyst. The reduction gives the complete 1st generation PPI dendrimer. These two steps (Michael addition and reduction) can be repeated to sequentially "grow" the dendrimer in successive generations until the starburst limit is reached. The reaction scheme for the 1st generation PPI is depicted in Figure 3.1.

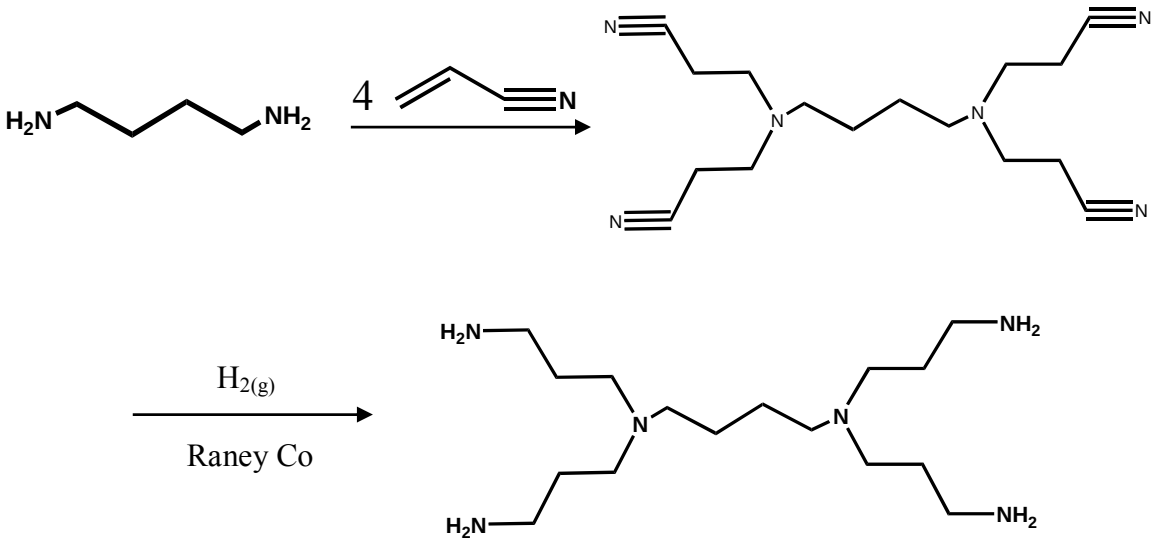

Figure 3. 1 Synthesis of 1st generation poly(propylene) imine dendrimer.

During the course of this research, it was necessary to synthesize two novel isotopically labeled dendrimers. Both of these dendrimers involved a labeled acrylonitrile; one had a ^{15}N terminus, while the other had a deuterium on the β-carbon. These are illustrated in Figure 3.2. Synthesis of these two dendrimers was achieved using a reaction scheme adapted from Meijer[4]

Figure 3. 2 Isotopically labeled acrylonitriles used in PPI synthesis.

and the procedure is detailed in the experimental section. The synthesized dendrimers are depicted in Figure 3.3. These synthesized dendrimers were analyzed in the same manner as the

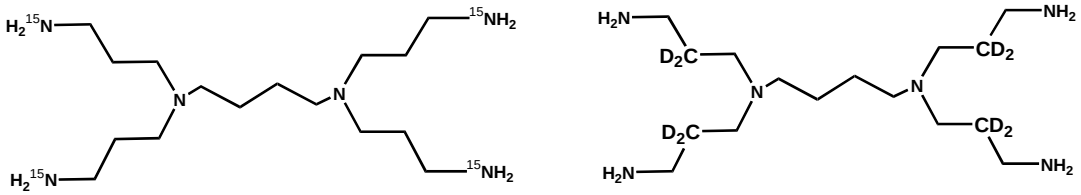

Figure 3. 3 1st generation ^{15}N (left) and ^{2}H (right) isotopically labeled dendrimers.

monoisotopic dendrimer. The ^{15}N labeled dendrimer was used to discriminate between interior nitrogens (those from the diaminobutane core) and exterior nitrogens (those from the acrylonitrile) during fragmentation. The ^{2}H labeled dendrimer was used to help identify possible fragmentation mechanisms that could involve a proton transfer from this deuterated carbon.

FRAGMENTATION

Isolation and fragmentation of the singly protonated 1st generation PPI dendrimer gives the fragmentation shown in Figure 3.4. Primary loss from the monoisotopic dendrimer is a fragment with a neutral mass of 131. The neutral fragment mass is found by subtracting the product mass (186.1) from the parent mass (317.2). Unambiguous identification of this fragment

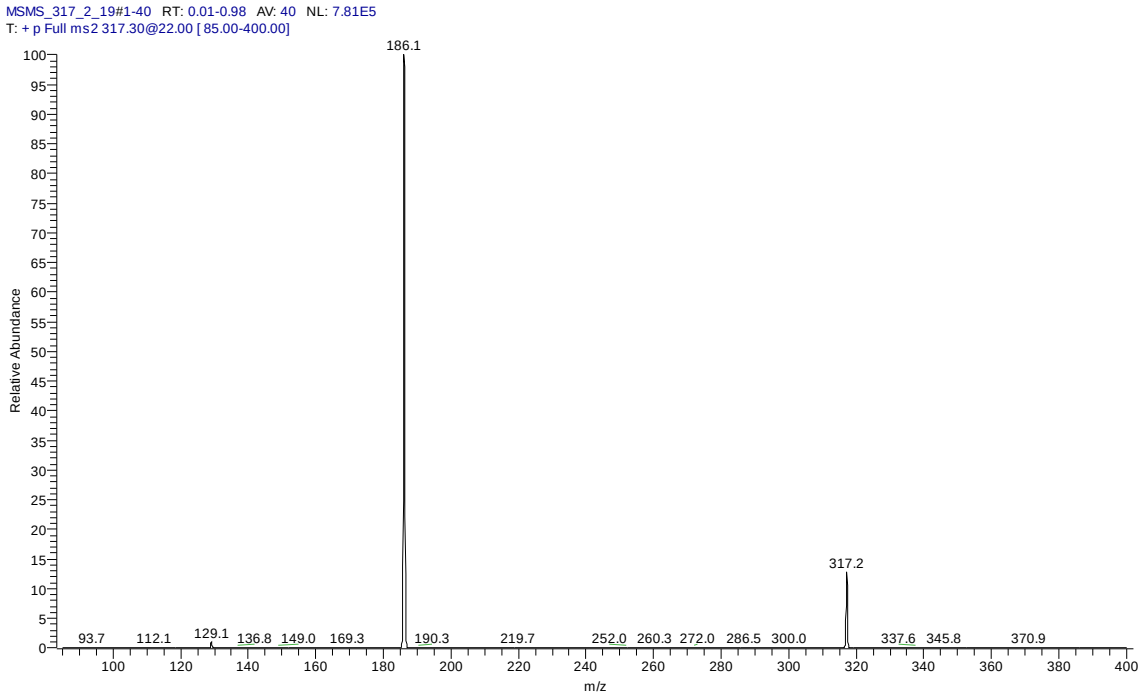

Figure 3. 4 Fragmentation of 1st generation PPI dendrimer at m/z = 317.2 leading to a dominant fragment at m/z = 186.1.

can be achieved through comparisons to the synthesized dendrimers. A comparison of the fragmentations of the ^{15}N labeled (m/z = 321) and the ^{2}H labeled (m/z = 325) can be seen in Figure 3.5. Comparing the primary fragment losses of 131 in the monoisotopic dendrimer, 133 in the ^{15}N labeled and 135 in the ^{2}H labeled, leads to identification of the fragment as an interior amine with its' two propyl amine arms, shown in Figure 3.6. Three possible mechanisms could lead to loss of this fragment; they are shown in Figure 3.7. The first, proposed by McLuckey[21], is an internal nucleophilic substitution resulting from the unprotonated tertiary amine attacking the carbon alpha to the protonation site. This results in a cyclic product with loss of neutral 131. The second is a charge remote mechanism involving a proton transfer to the leaving group and formation of a double bond (ene) product. The third proposed mechanism involves a hydride transfer to the carbon alpha to the protonation site and formation of an imine. This imine

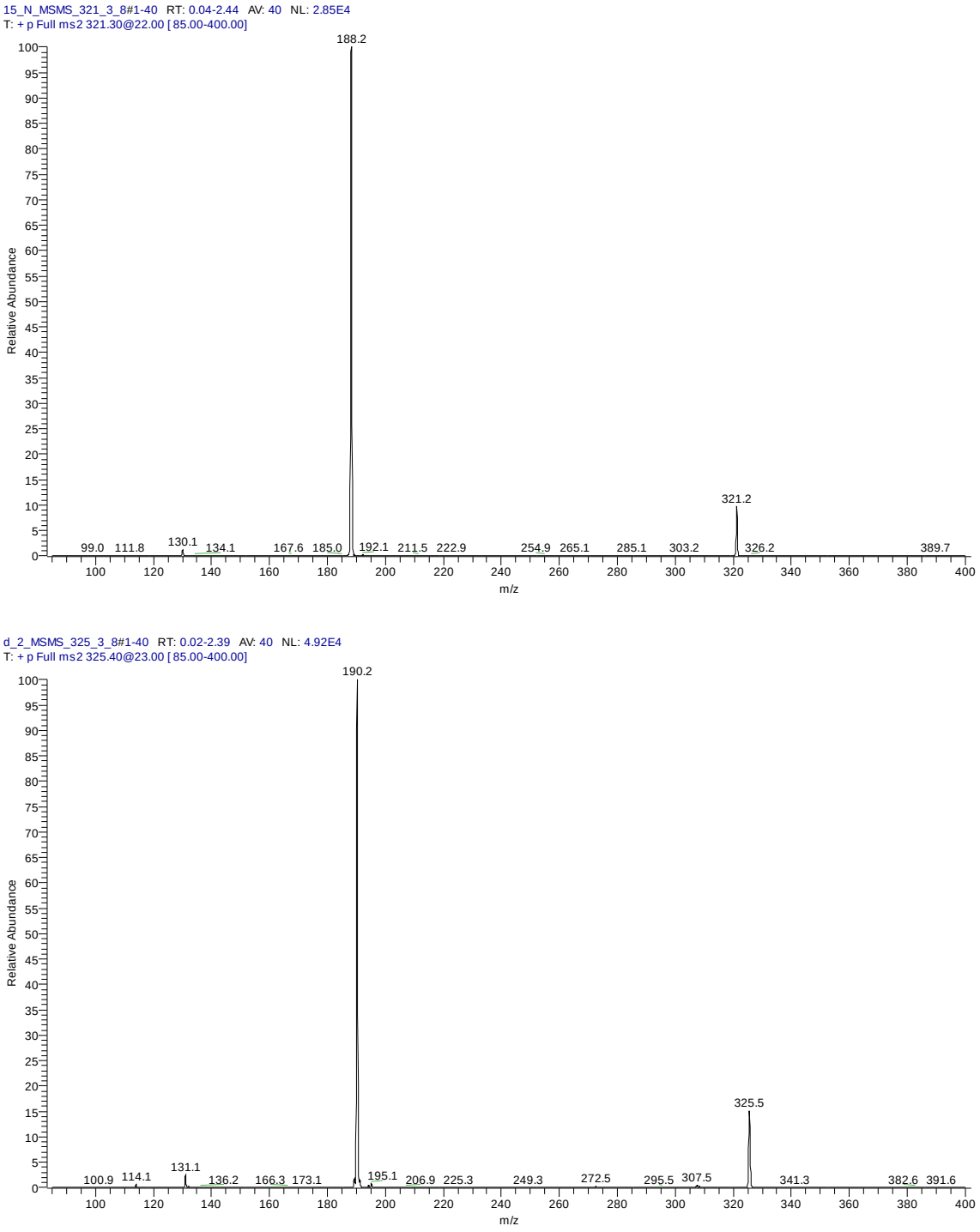

Figure 3. 5 Fragmentation comparison of ^{15}N labeled dendrimer (top) at m/z = 321.2 leading to a product ion at m/z = 188.2 (neutral loss of 133) and the ^{2}H labeled dendrimer (bottom) at m/z = 325.5 leading to a product ion at m/z = 190.2 (neutral loss of 135).

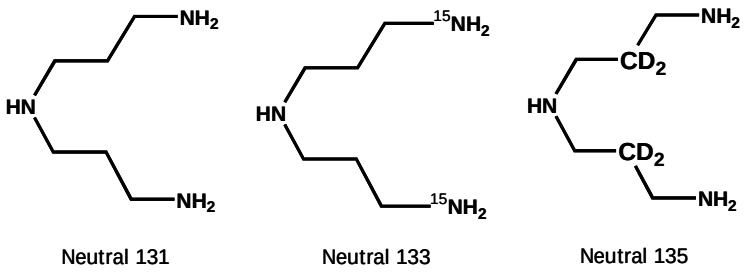

Figure 3. 6 Identification of primary fragment from monoisotopic (neutral 131), ^{15}N labeled (neutral 133) and ^{2}H labeled (neutral 135) dendrimers.

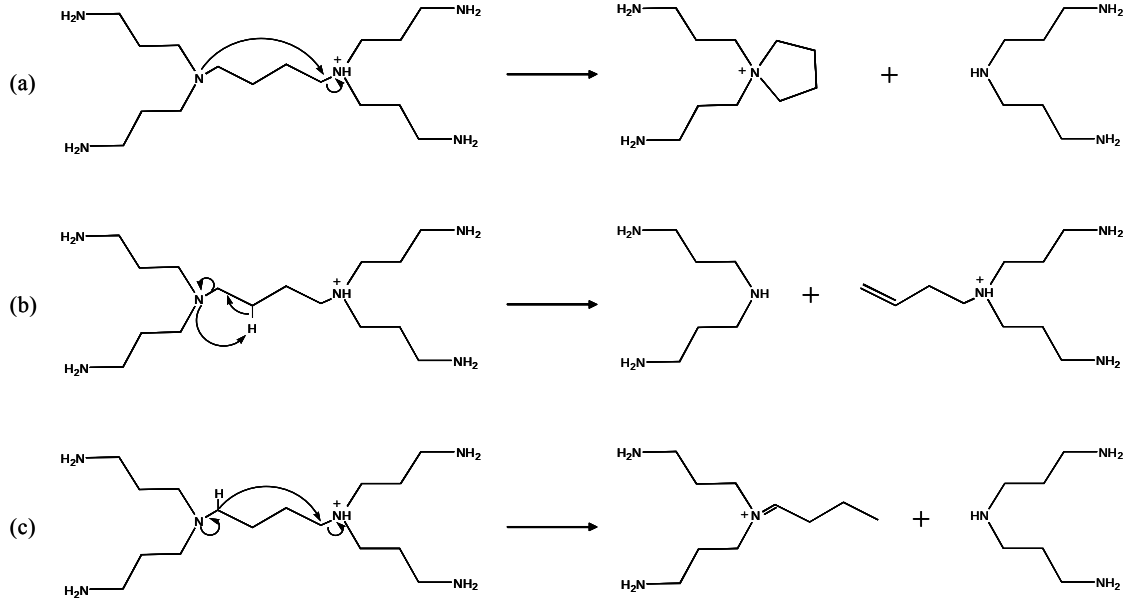

Figure 3. 7 Proposed mechanisms for fragmentation: (a) nucleophilic substitution, (b) elimination to form double bond (ene), (c) hydride transfer and formation of imine.

formation was identified by Bochoux when studying α,ω-aminoalcohols in the gas-phase.[22] All three of these mechanisms result in loss of neutral 131 and the charged product. These charged products, however, are indistinguishable in the mass spectrometer.

In an attempt to determine the dominant mechanism, the thermochemistry of the products

and their respective transition states were calculated. The relative Gibbs free energy profile is shown in Figure 3.8. As shown in the figure, the substitution mechanism has the lowest relative energy transition barrier and should dominate. Another important point is the intermediate transition state in the substitution mechanism. In order for the attacking nitrogen to get into the proper position for the substitution, the butane backbone must twist. This twist will be important when discussing the metal complexed species.

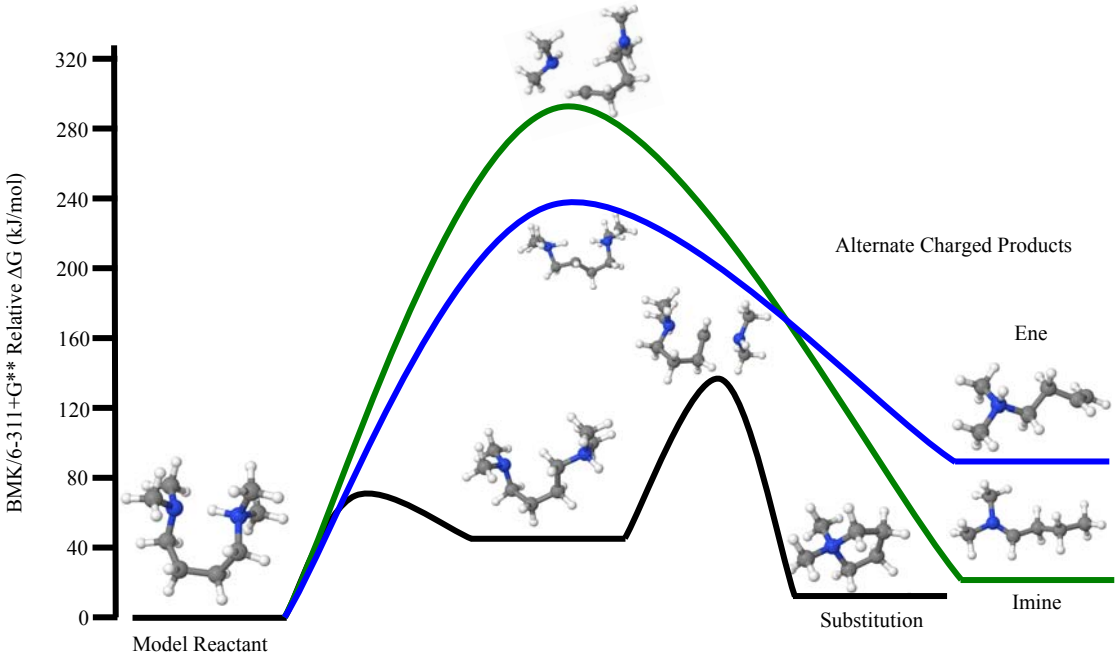

Figure 3. 8 Relative Gibbs free energy profiles of three proposed mechanisms starting from a tetramethyl diaminobutane model reactant and showing the free energy transition states and final products.

Having identified the structure of the primary fragment at m/z = 186, the fragmentation of this ion is shown in Figure 3.9. The primary loss is a neutral 57 and gives the charged product at m/z = 129. This fragmentation can occur through two possible mechanisms: substitution or elimination. These are illustrated in Figure 3.10. The substitution mechanism occurs as a primary nitrogen attacks the carbon alpha to the quaternary amine and transfers a proton giving a loss of 57 and the charged product. Alternatively, a proton transfer and formation of the double

bond gives the same loss of 57. With this fragmentation, the isotopically labeled PPI's provide evidence for not only the fragment, but also the mechanism of the loss. The ^{15}N labeled

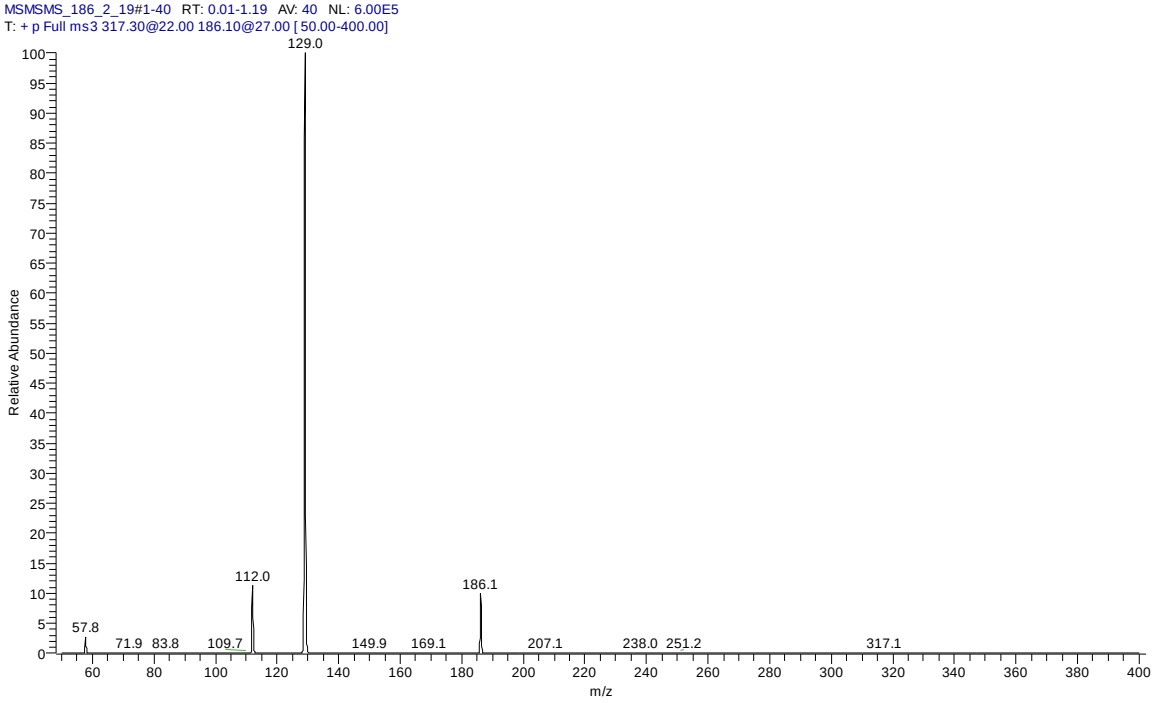

Figure 3. 9 Fragmentation of m/z = 186.1, showing a dominant product ion at m/z = 129 and minor product ions at m/z = 112.0 and 57.8.

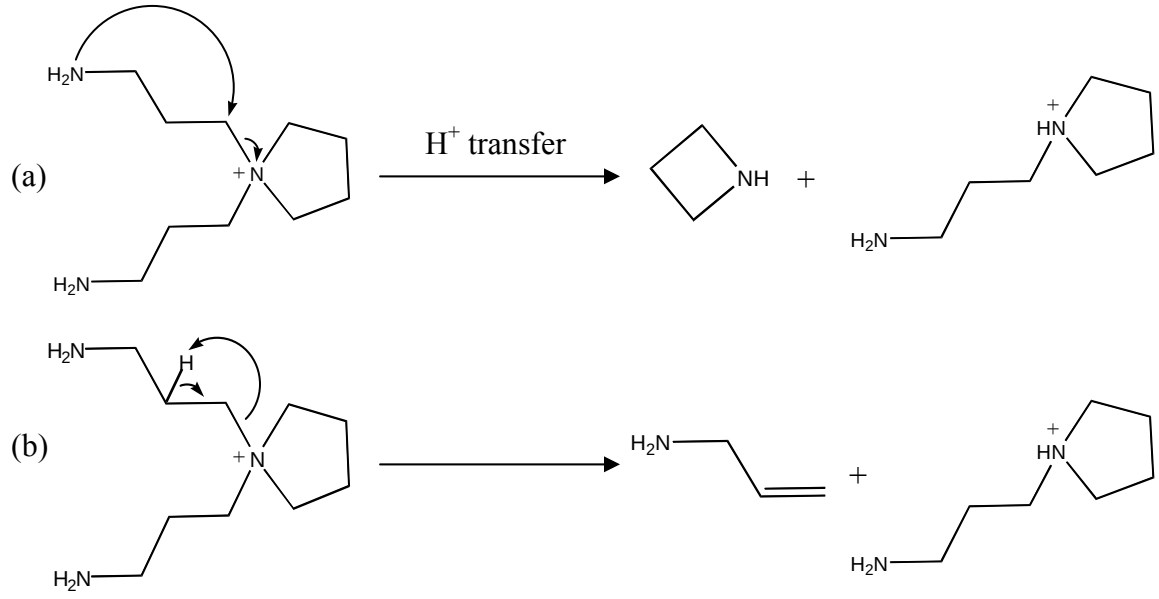

Figure 3. 10 Possible fragmentation mechanisms for species at m/z = 186: (a) nucleophilic substitution and (b) elimination.

dendrimer confirms that it is an exterior nitrogen in the leaving group. The ^{2}H labeled dendrimer confirms that there is no deuterium transfer between the β-carbon and the interior quaternary amine that would occur in the elimination mechanism; providing evidence that the substitution mechanism dominates in this case as well. There is also evidence in the small peak at m/z = 58 (see Figure 3.9). After the substitution there is a proton migration from the leaving group to the tertiary amine. If the proton migrates, the result in the dominant product at m/z = 129; if it does not, the product would be at m/z = 58.

Examining the isolation and fragmentation of m/z = 129 (Figure 3.11), the major loss is a neutral 17 (NH_3). Given the neutral loss of the previous fragment, one would expect that a loss of 57 would be dominant, or at least competitive, but the loss of 17 is clearly dominant. The evidence from the labeled fragmentations shows that the exterior nitrogen is lost (loss of neutral 18 in ^{15}N labeled) and that the two deuteriums stay with the charged fragment. Examining the

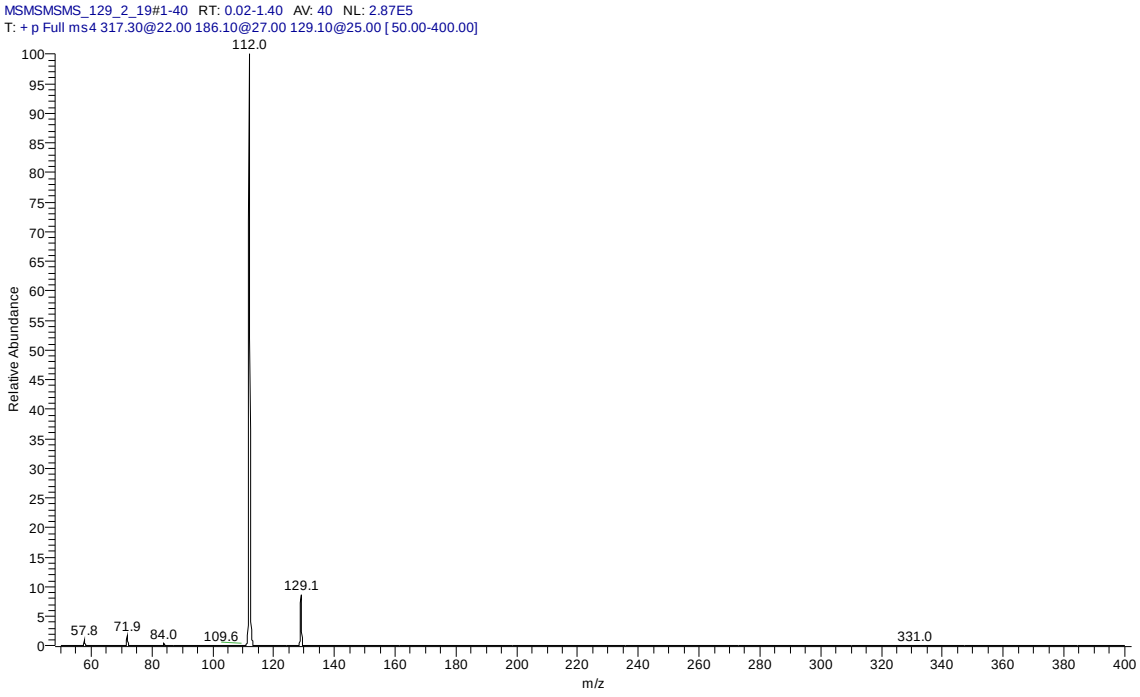

Figure 3. 11 Fragmentation of m/z = 129 giving dominant product at m/z = 112.0 and minor products at m/z = 57.8, 71.9 and 84.0.

possible mechanisms, shown in Figure 3.12, the substitution toward the inside would give peaks at m/z = 58 or 72 depending on which fragment retained the proton. The dominant mechanism, however, requires a migration of the proton from the tertiary amine to the exterior primary amine and then nucleophilic attack by the interior nitrogen on the β-carbon giving loss of ammonia.

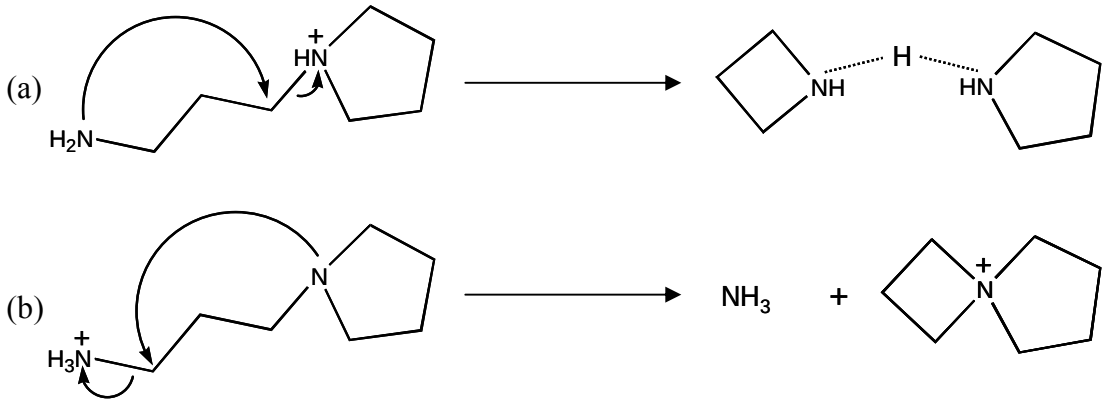

Figure 3. 12 Possible fragmentation mechanisms for m/z = 129: (a) nucleophilic substitution to the "inside" and (b) migration of proton and nucleophilic substitution to the "outside."

Finally, the fragmentation of m/z = 112 gives a major peak at m/z = 84 and a minor peak at m/z = 70 (Figure 3.13). These two fragments are formed by fragmentation in either ring that leads to a loss of neutral ethene or propene and the two charged products, shown in Figure 3.14.

Based on the evidence, a full fragmentation scheme, Figure 3.15, shows that the fragmentation of the 1st generation PPI dendrimer fragments mainly thorough substitution mechanisms. This scheme requires substantial flexibility in the molecule and this flexibility will come into play when discussing the metal-complexed species.

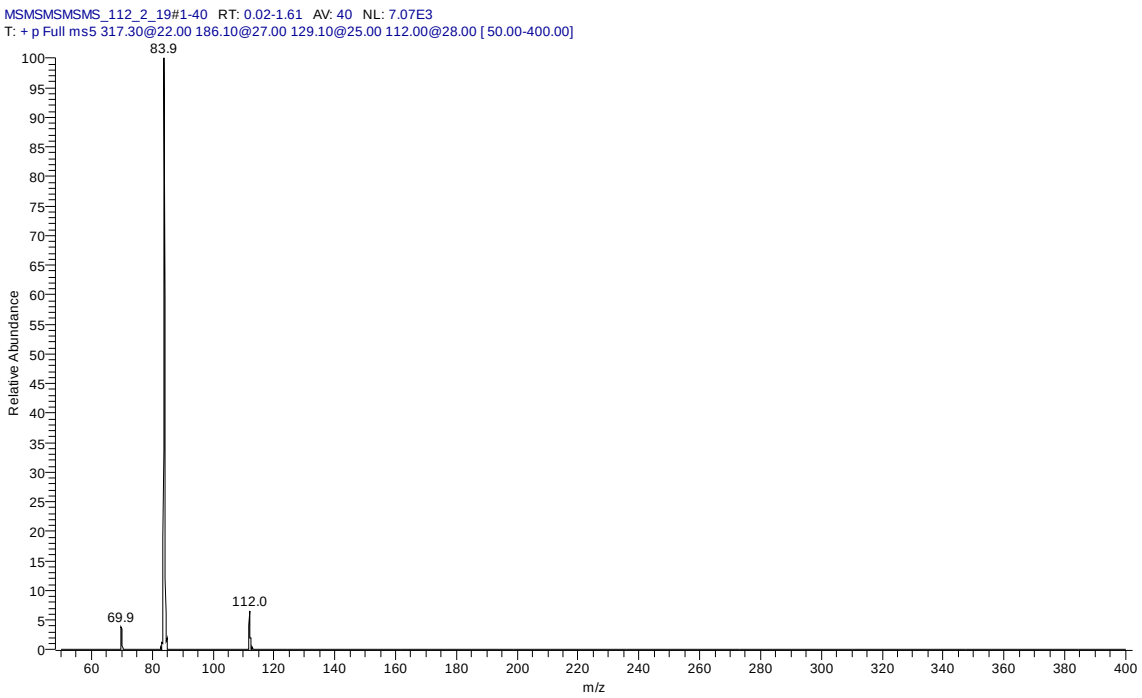

Figure 3. 13 Fragmentation of m/z = 112 giving a major product ion at m/z = 83.9 and a minor product ion at m/z = 69.9.

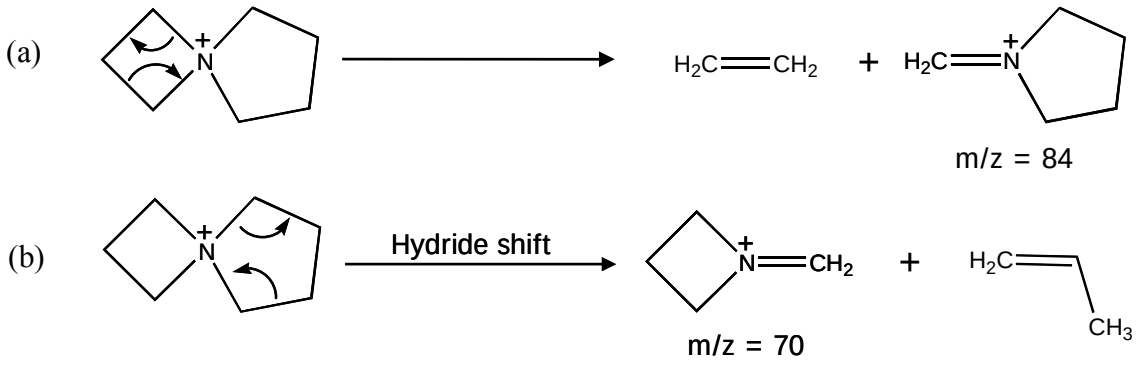

Figure 3. 14 Possible fragmentations for m/z = 112 giving product ions at (a) m/z = 84 and (b) m/z = 70, depending on which ring fragments.

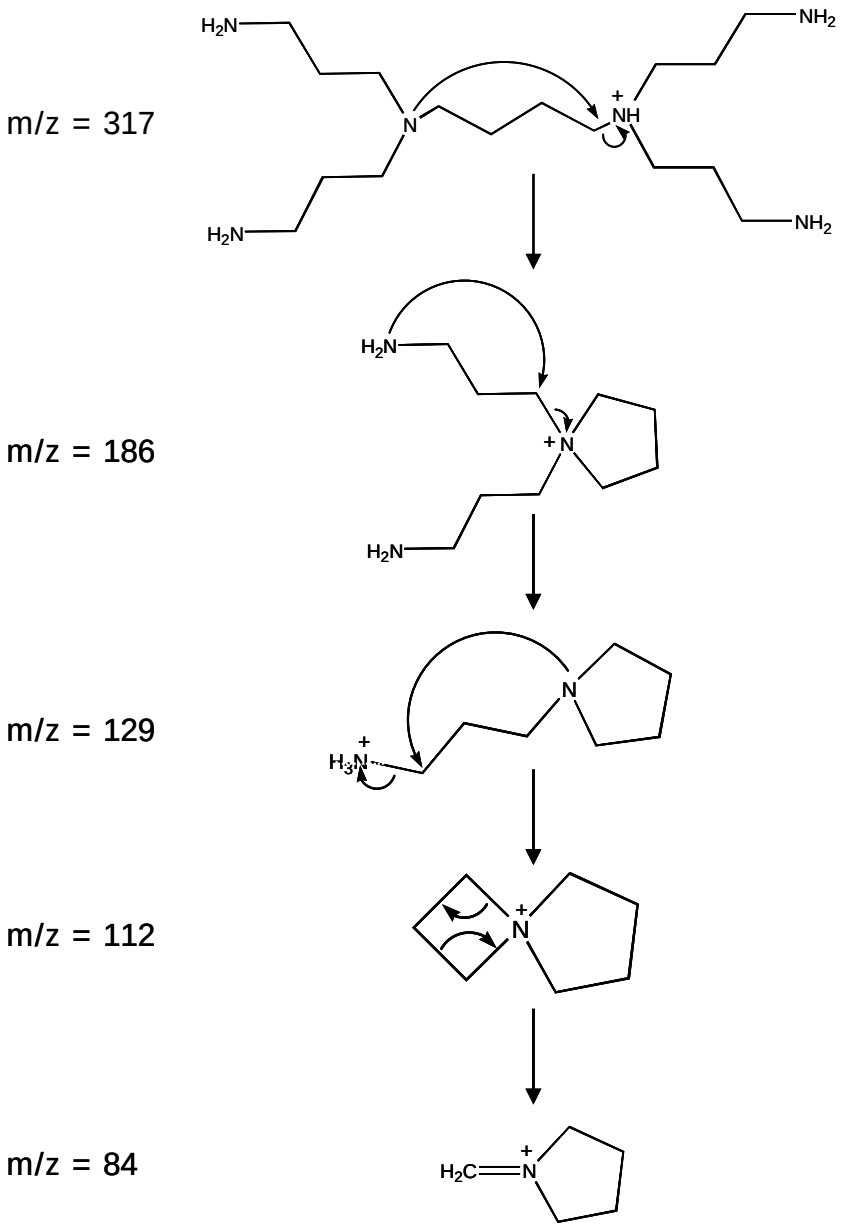

Figure 3. 15 Fragmentation scheme of 1st generation PPI dendrimer, showing prevalence of nucleophilic substitution mechanisms.

CHAPTER FOUR: PPI-METAL COMPLEXES

GENERAL

PPI-metal complexes were formed in solution and analyzed in a similar manner to the protonated species. Analyzed complexes were charge-reduced, meaning that they are a divalent metal with a deprotonated dendrimer for a one-plus complex $[M(PPI - H^+)]^+$, where M is the two-plus metal.

PPI-ZINC

The fragmentation of the Zn-PPI complex at m/z = 379 is shown in Figure 4.1. In comparison with the protonated dendrimer, this fragmentation is much more complex. Multiple fragmentations occur. Primary neutral losses are 17, 57, 131 and 185; the first three being losses that are seen in the protonated species. In order to positively identify these fragments, a

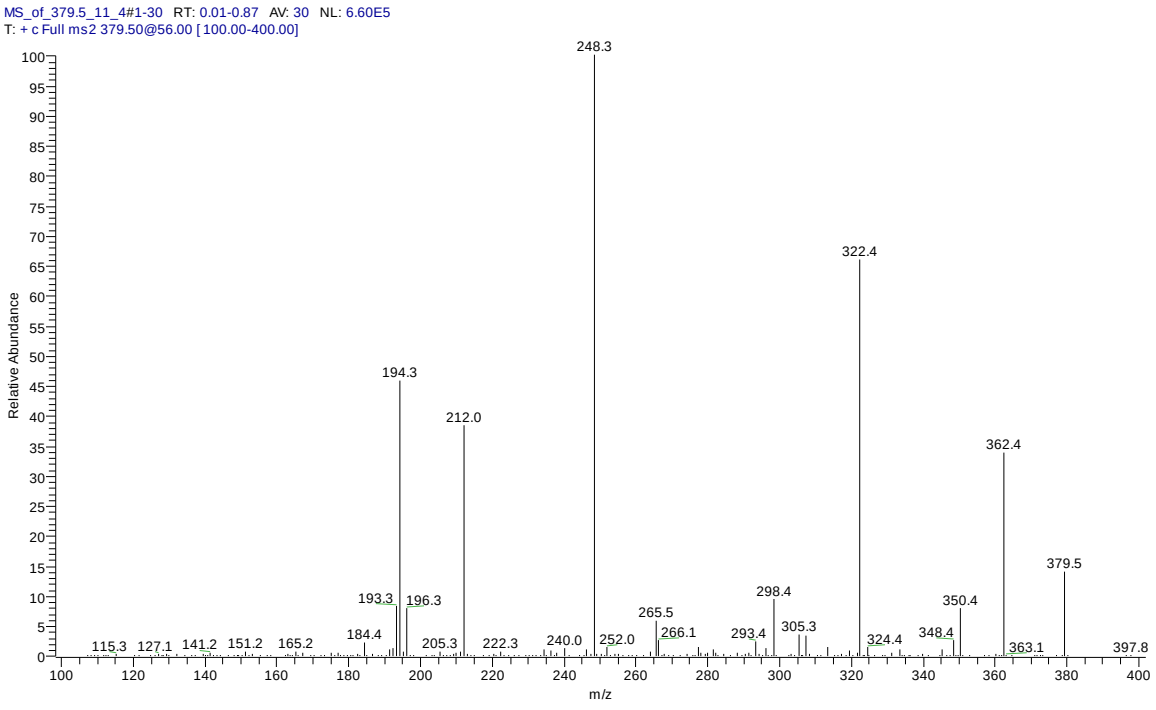

Figure 4. 1 Fragmentation of Zn-complexed PPI dendrimer at m/z = 379.5 showing multiple losses upon initial fragmentation. Note the increased complexity of fragmentation when compared to the protonated species.

comparison fragmentation with the ^{15}N-labeled dendrimer is shown in Figure 4.2 and a comparison table with identified fragments is given in Table 4.1.

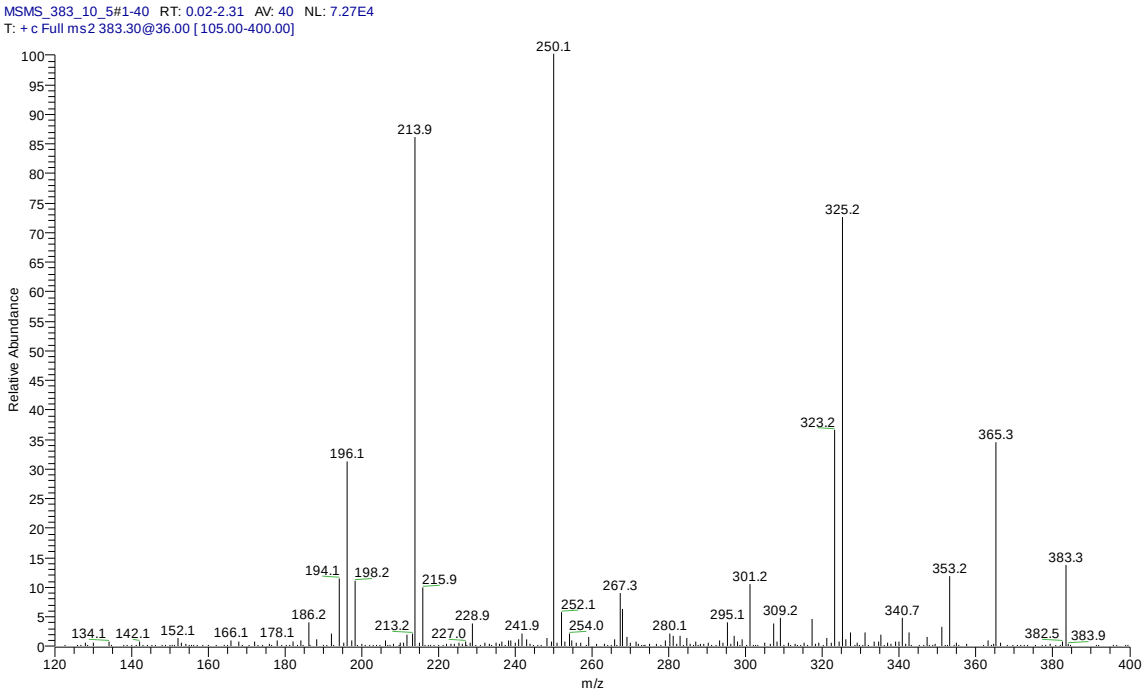

Figure 4. 2 Fragmentation of ^{15}N labeled PPI complexed with divalent Zinc at m/z = 383.3.

Table 4. 1 Comparison of monoisotopic and ^{15}N labeled Zn-PPI complexes.

Species	Parent (m/z)	Fragment (m/z)	Neutral loss	Identification
Monoisotopic Zn-PPI	379.5	362.4	17.1	NH_3
		322.4	57.1	C_3H_7N
		248.3	131.2	$C_6H_{17}N_3$
		194.3	185.2	$C_{10}H_{23}N_3$
^{15}N-exterior labeled Zn-PPI	383.3	365.3	18.0	$^{15}NH_3$
		325.2	58.1	$C_3H_7{}^{15}N$
		250.1	133.2	$C_6H_{17}N^{15}N_2$
		196.1	187.2	$C_{10}H_{23}N^{15}N_2$

The comparison confirms the identification of the fragments, but to identify the mechanism, the conformation of the complex must be known. For this purpose the relative energy of several Zn-PPI complex conformations were calculated; this is given in Figure 4.3. As

seen in the figure, the lowest energy conformation (the structure on the far left) is with the Zinc complexed to a tertiary nitrogen, its two associated primary nitrogens and a primary nitrogen from the opposite side of the dendrimer in a pseudo-tetrahedral arrangement. The highest in energy has all four primary nitrogens complexed to the metal. This lowest energy conformation is the probable one as the complex is isolated in the mass spectrometer. Given this information, probable fragmentation mechanisms can be proposed.

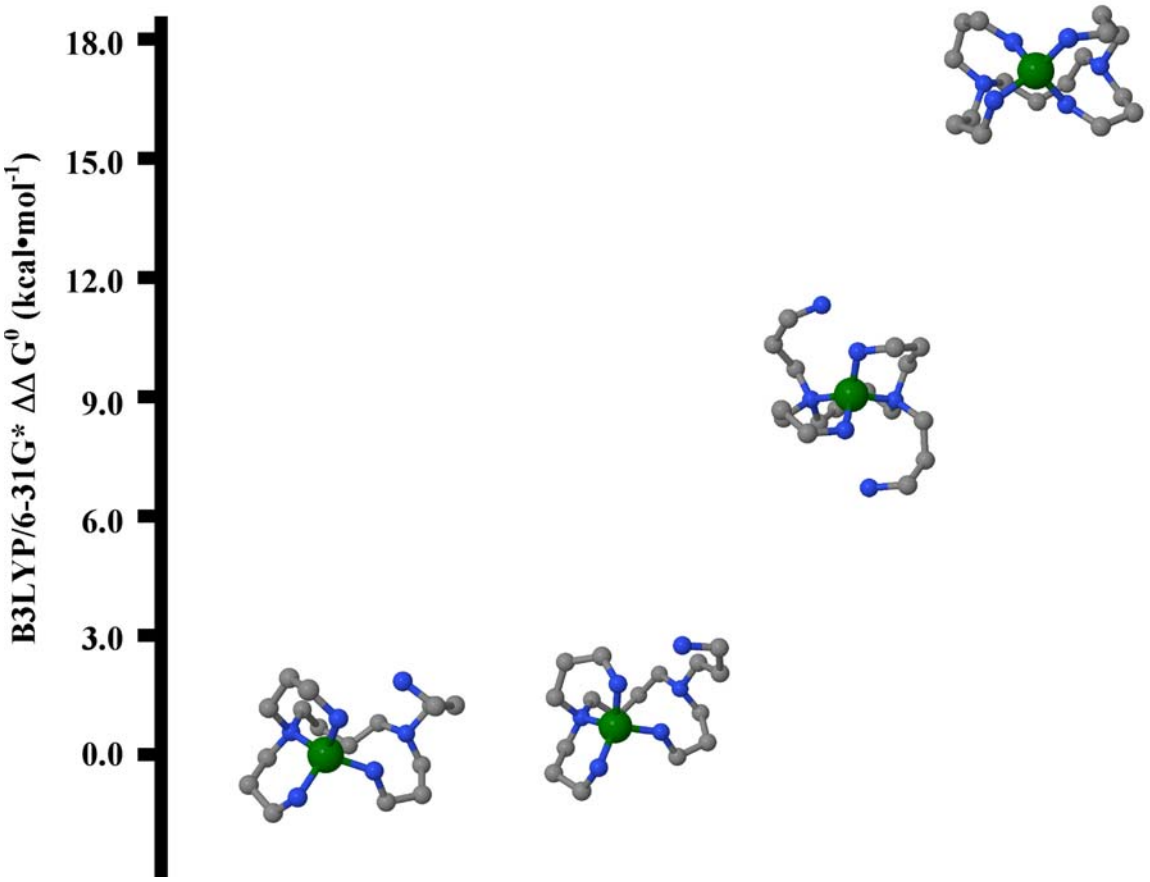

Figure 4. 3 Relative free energy calculations of four Zn-PPI dendrimer conformations; increasing relative energy moving to the right in the picture.

Recall that in the protonated species, the dominate substitution mechanism involved an intermediate transition state with the butane backbone twisting to reach the proper orientation. This twist is unavailable to the metal complexed species because the dendrimer is being "locked"

into one conformation. Therefore, while there are similar losses in comparison to the protonated dendrimer, the mechanism is different; the elimination mechanism appears to dominate. Evidence to support this comes from the fragmentation.

There are two possible fragmentations within the butane core and they are shown in Figure 4.4. The mechanisms are termed elimination "far" and elimination "near," the direction indicative of the position relative to the deprotonation site, in this case the upper right primary nitrogen. Elimination at the "far" site gives a neutral loss of 131 and a charged product at m/z =

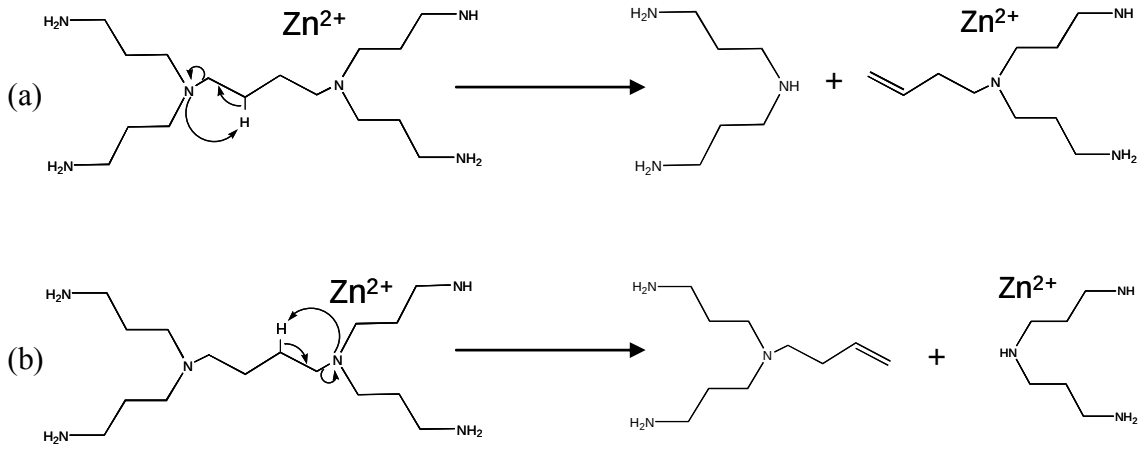

Figure 4. 4 Fragmentations of Zn-PPI complex within the butane core: (a) elimination "far" and (b) elimination "near." The charged product ion in (b) picks up a neutral water adduct upon isolation and storage in the ion-trap; the charged product ion in (a) does not.

248, whereas elimination "near" gives a neutral loss of 185 and a charged product at m/z = 194. This fragment at m/z = 194, upon isolation and storage in the ion-trap, picks up a neutral water adduct; the m/z = 248 ion does not. It is hypothesized that the Zinc-complex has a strong thermodynamic need to complete the coordination shell and, in the m/z = 194 case, the complex has three nitrogens and completes the shell with a water molecule; the m/z = 248 has three

nitrogens and the pi system of the double bond that associates with the metal to complete the shell.

Examining and comparing the multiple unlabeled and labeled Zn-PPI fragmentations, a full fragmentation scheme can be developed and is shown in Figure 4.5.

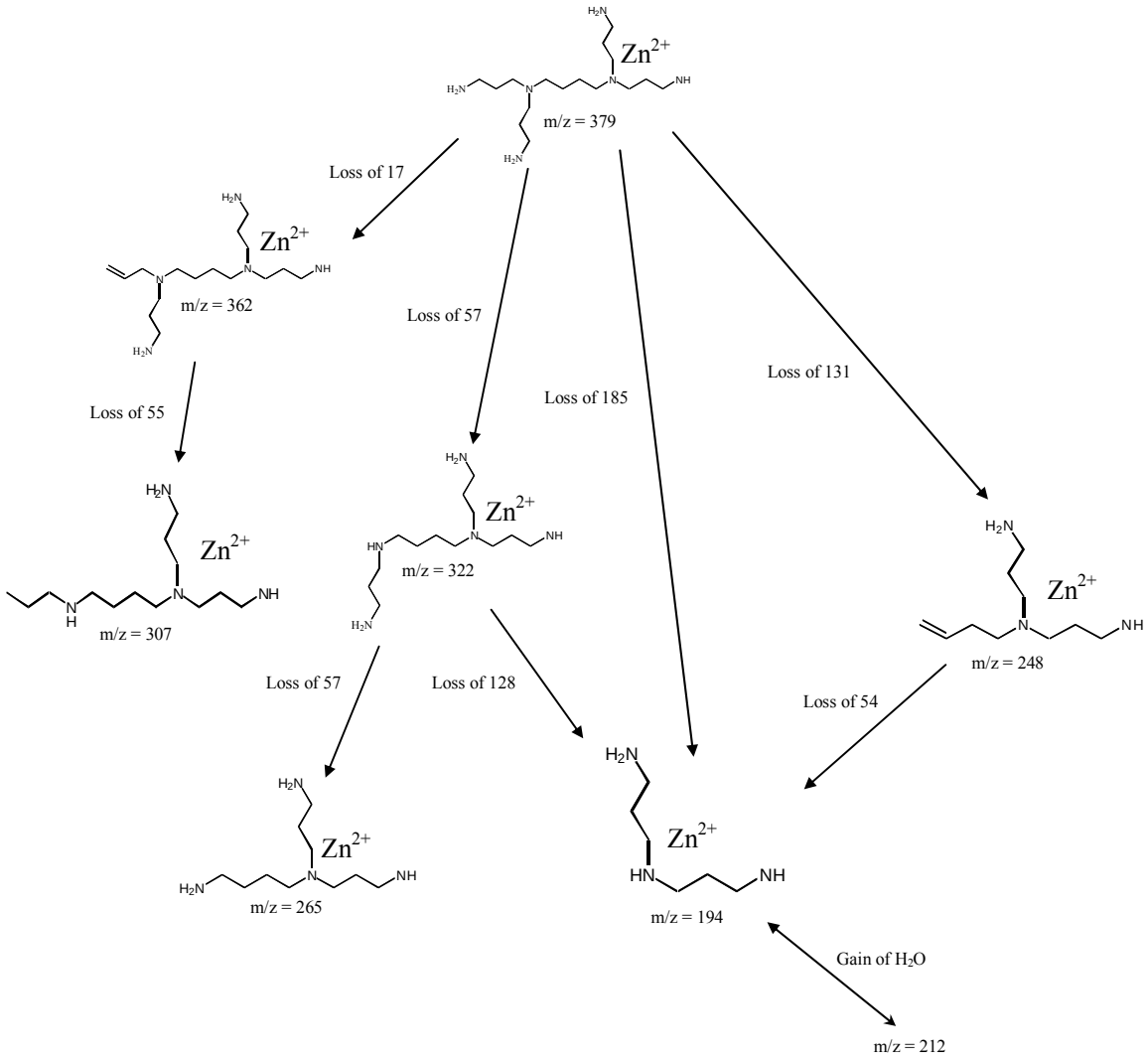

Figure 4. 5 Fragmentation scheme of Zn-PPI complex showing neutral losses and resulting charged fragments.

PPI-COBALT

The Co-PPI dendrimer and the ^{15}N-labeled complex fragmentations are shown in Figure 4.6. Many fragmentations occur, including neutral losses of 17, 57, 131, and 185 like those

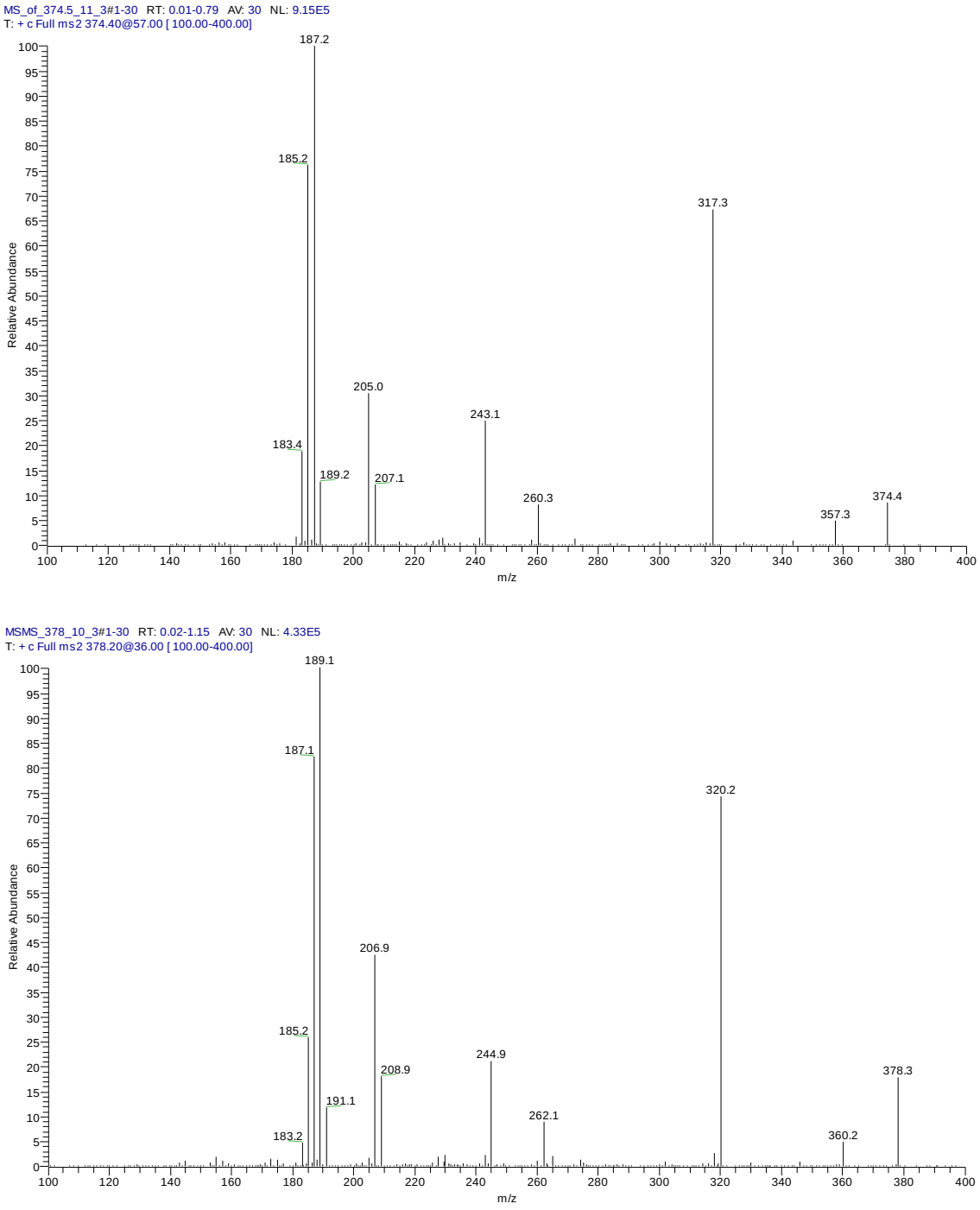

Figure 4. 6 Comparison of monoisotopic (top at m/z = 374.4) and ^{15}N labeled (bottom at m/z = 378.3) Co-PPI fragmentation.

previously seen in the Zn-PPI complex. Also, the addition of water to the fragment at m/z = 189 is comparable. The Co-PPI complex, however, shows evidence for metal-catalyzed dehydrogenation after the neutral loss of the 185 fragment. The water adduct complexes with only the first of these ions, giving more evidence that the pi system of the dendrimer is associating with the metal to fill vacant coordination sites.

In addition, a neutral loss unique to the Cobalt complex occurs from the fragmentation of m/z = 243. This fragment has lost a neutral 131 in a proposed elimination mechanism leaving the butane core with a terminal double bond. The fragmentation of this m/z = 243 goes exclusively to m/z = 187, that then picks up a neutral water adduct. The neutral loss of 56 comes from the butane core. This loss occurs through a proposed elimination mechanism involving a proton transfer. In the Zinc complex, this equivalent fragmentation occurs with the proton transferring **from** the leaving group resulting in a neutral loss of 54, however, in the Cobalt complex the proton transfers **to** the leaving group, leaving a double bond on the metal containing dendrimer. Clearly the metal association to the dendrimer influences the fragmentation.

A full fragmentation scheme is given in Figure 4.7.

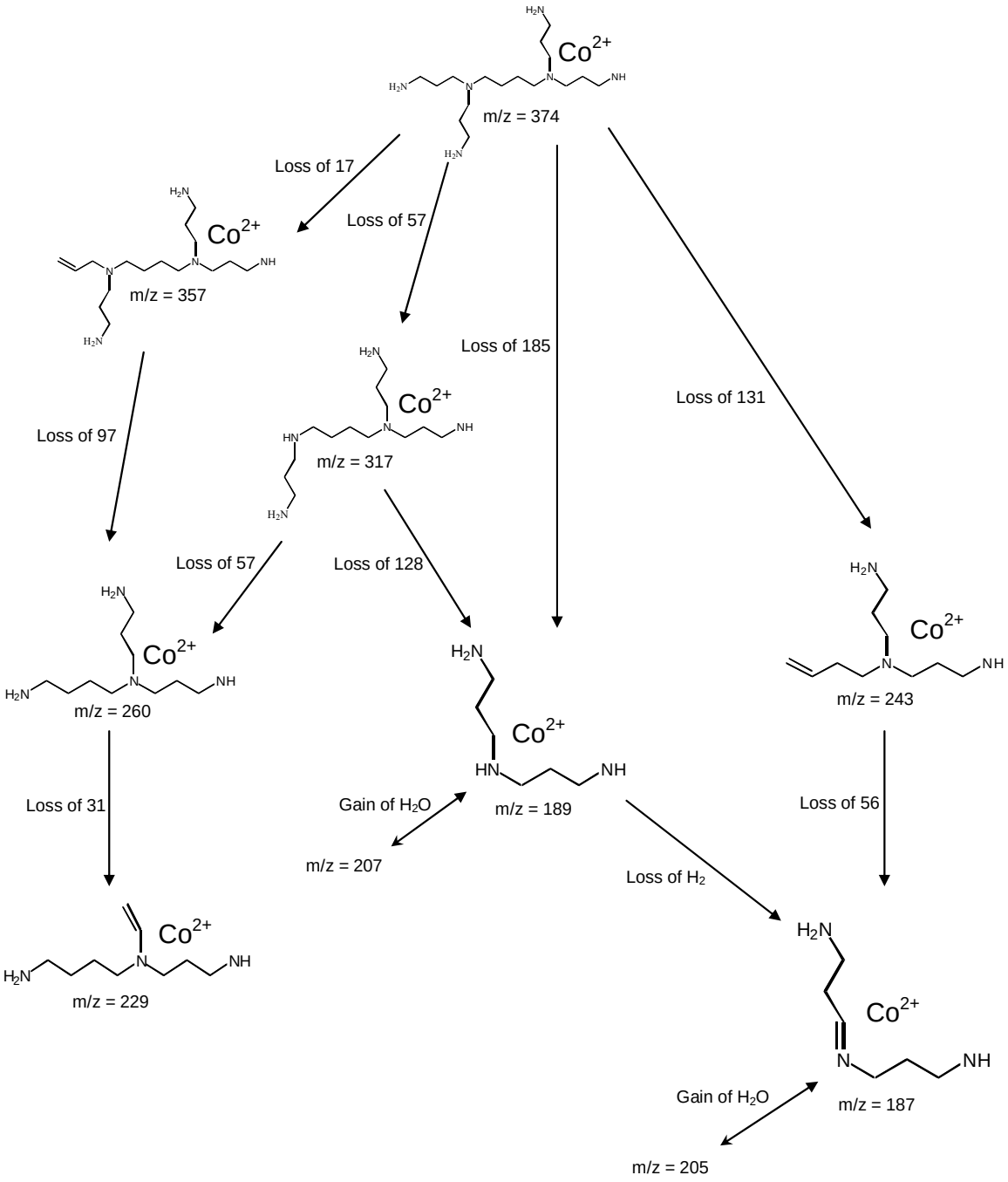

Figure 4. 7 Fragmentation scheme of Co-PPI complex showing neutral losses and resulting charged fragments.

PPI-NICKEL

The fragmentation scheme of the PPI-Nickel complex is shown in Figure 4.8. The primary neutral losses include 17, 57, 131 and 185, like those previously seen. Interestingly, there appears to be no addition of water to the charged product at m/z = 188; a fragment that has picked up water in the Zinc and Cobalt species.

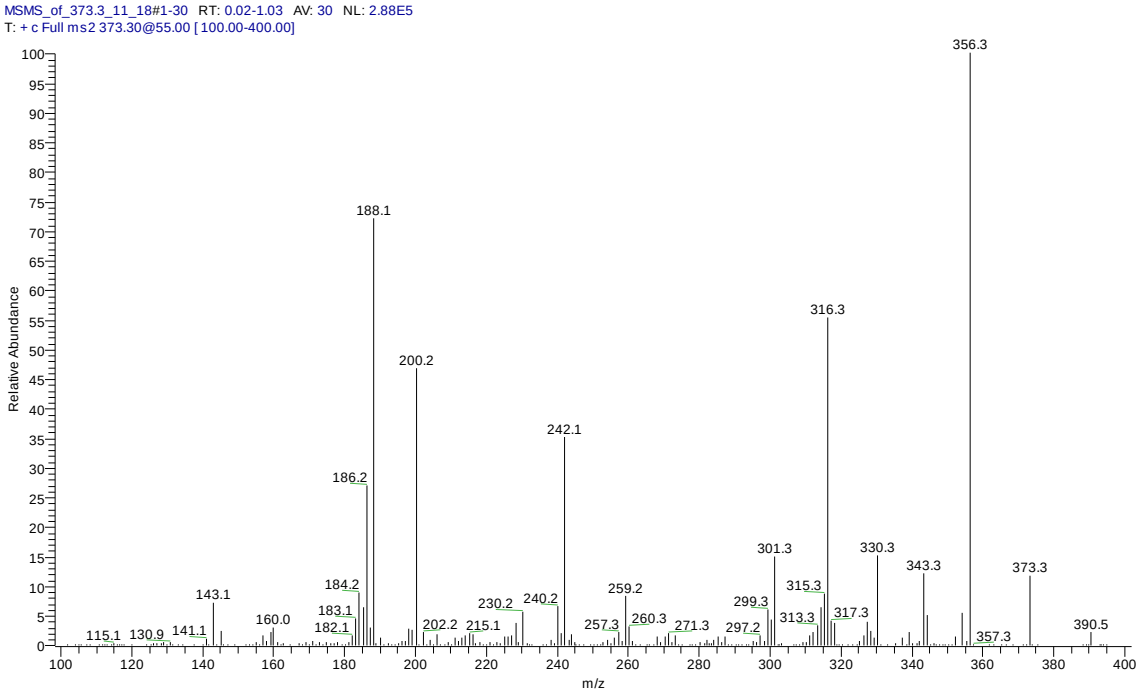

Figure 4. 8 Fragmentation of Ni-complexed PPI dendrimer at m/z = 373.3.

The peak at m/z = 200 results from a neutral loss that is not seen in the other species studied. Upon further study, this charged species is the result of a fragmentation from the ion at m/z = 242; this ion being the result of a fragmentation from the ion at m/z = 316. This m/z = 316 species has lost one exterior arm. Examining the fragmentation of the resultant species, it is possible to determine the structure of the dendrimer on the metal.

There are two possible fragmentations from the species at m/z = 316 leading to an ion at m/z = 242. Upon comparison with the ^{15}N labeled dendrimer, this neutral loss of 74 in the

monoisotopic dendrimer is a neutral 75 in the labeled species, meaning that the neutral loss contains one exterior nitrogen. There are two possibilities for the neutral loss of 74 from this m/z = 316 complex; one is from an exterior arm and the other is from an interior arm. These are illustrated in Figure 4.9. Although these resulting ions at m/z = 242 are indistinguishable in the mass spectrometer, the structure can be inferred from its further fragmentation. The subsequent

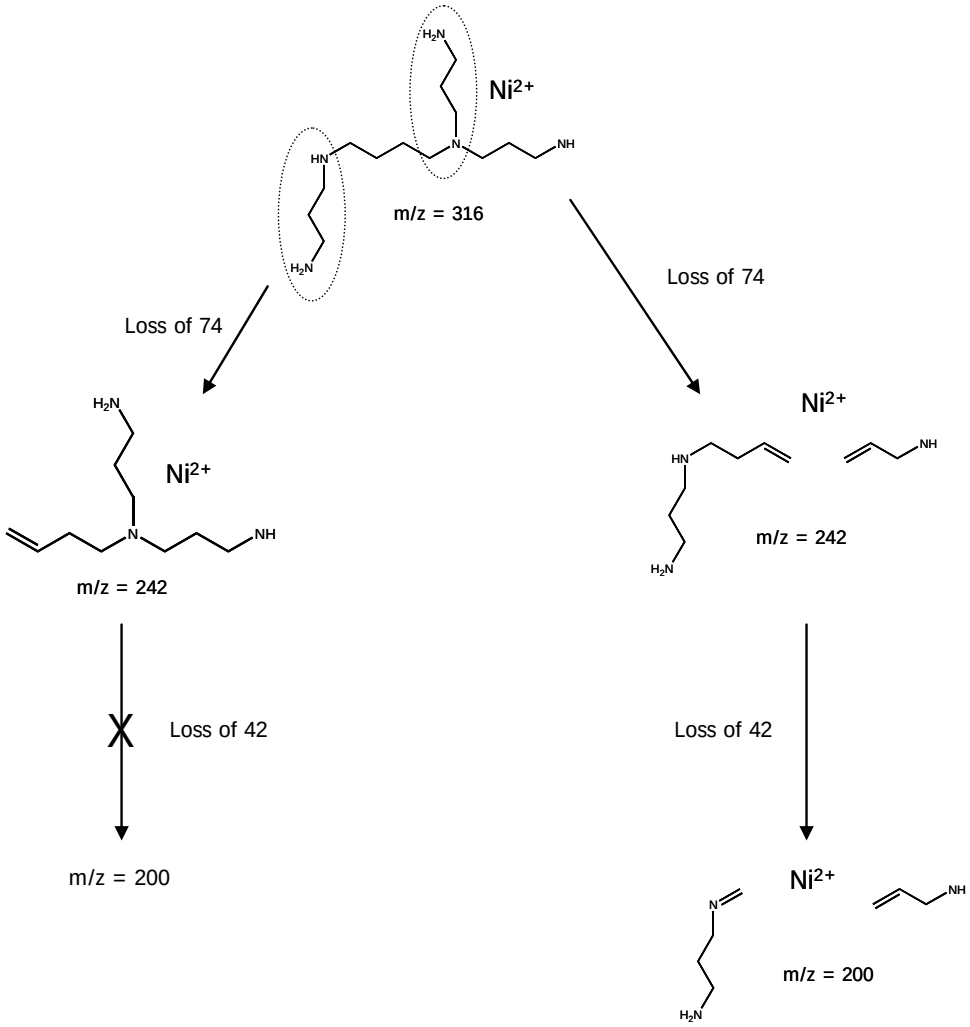

Figure 4. 9 Possible fragmentations of m/z = 316 showing two different losses of neutral 74. The subsequent loss of neutral 42 provides evidence for the structure of the dendrimer.

loss from m/z = 242 is a neutral 42 in both the monoisotopic and labeled complexes, meaning that the fragment comes from the butane core. The neutral 42 is most likely propene. Formation

of this neutral loss requires the transfer of a proton from the atom beta to the recipient carbon on the leaving group and formation of a double bond on the metal containing dendrimer. Examining the possible structures for m/z = 242, only the one that had lost the interior fragment has a proton in the site beta to the recipient carbon. It is also worth noting that the resulting species (m/z = 200) does not pick up a neutral adduct upon isolation and storage, suggesting that the dendrimer is capable of completing the coordination shell. The fragmented dendrimer would be capable of reorganizing its association with the metal to complete the coordination.

The complete fragmentation scheme for the PPI-Nickel complex is shown in Figure 4.10. There is also evidence for a neutral loss of 55 in the complex that has lost ammonia (m/z = 356); this is similar to the Zn-PPI complex.

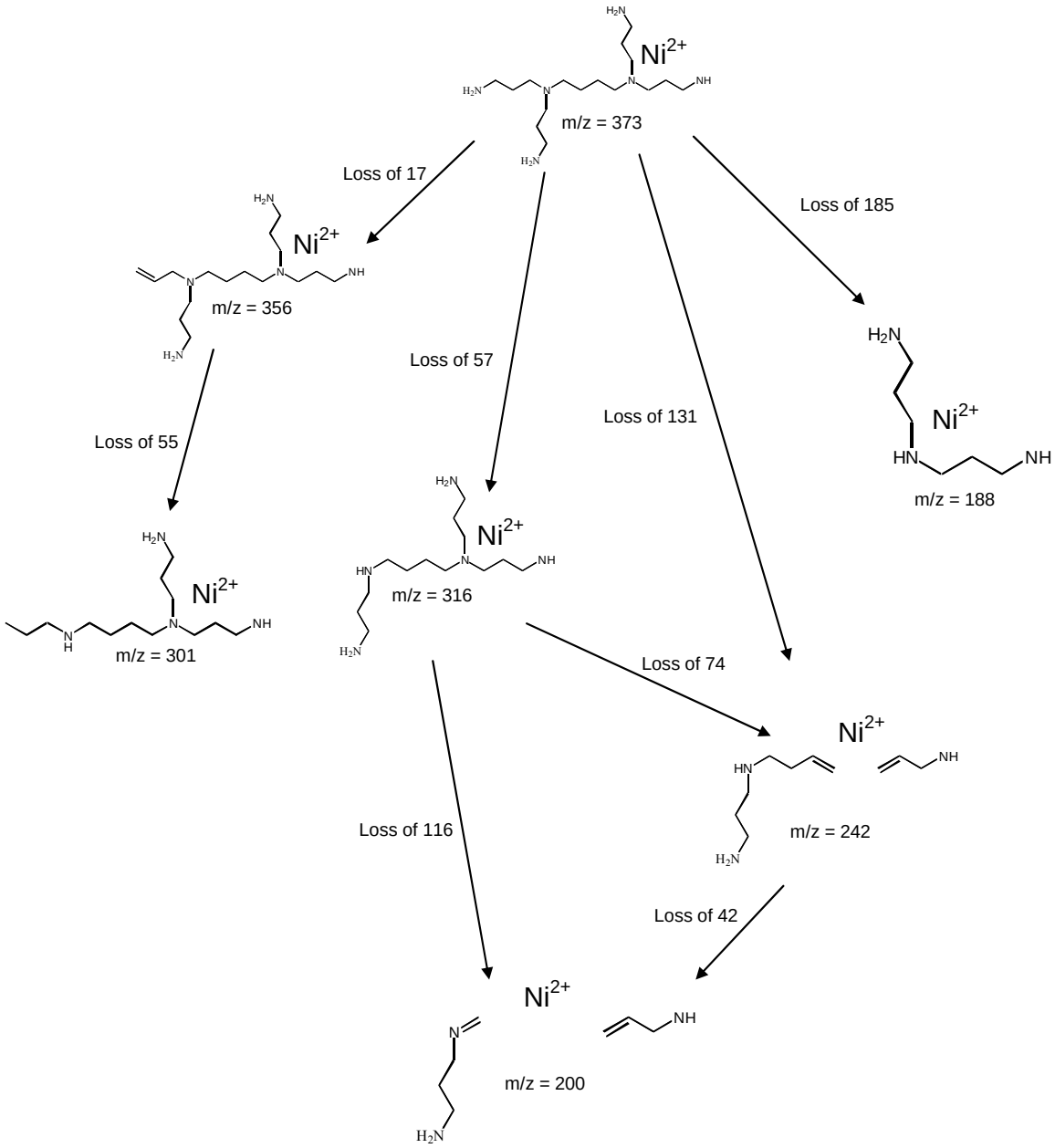

Figure 4. 10 Fragmentation scheme of Ni-PPI complex showing neutral losses and resulting charged fragments.

PPI-COPPER

The PPI-Cu complex fragmentation is considerably different than the previous metals studied. The initial fragmentation, seen in Figure 4.11, shows neutral losses of 58, 129 and 186. In order to account for these losses, like in the case of the neutral 58 and 186 losses that are one mass unit difference from the other metals, a radical mechanism was needed. In the case

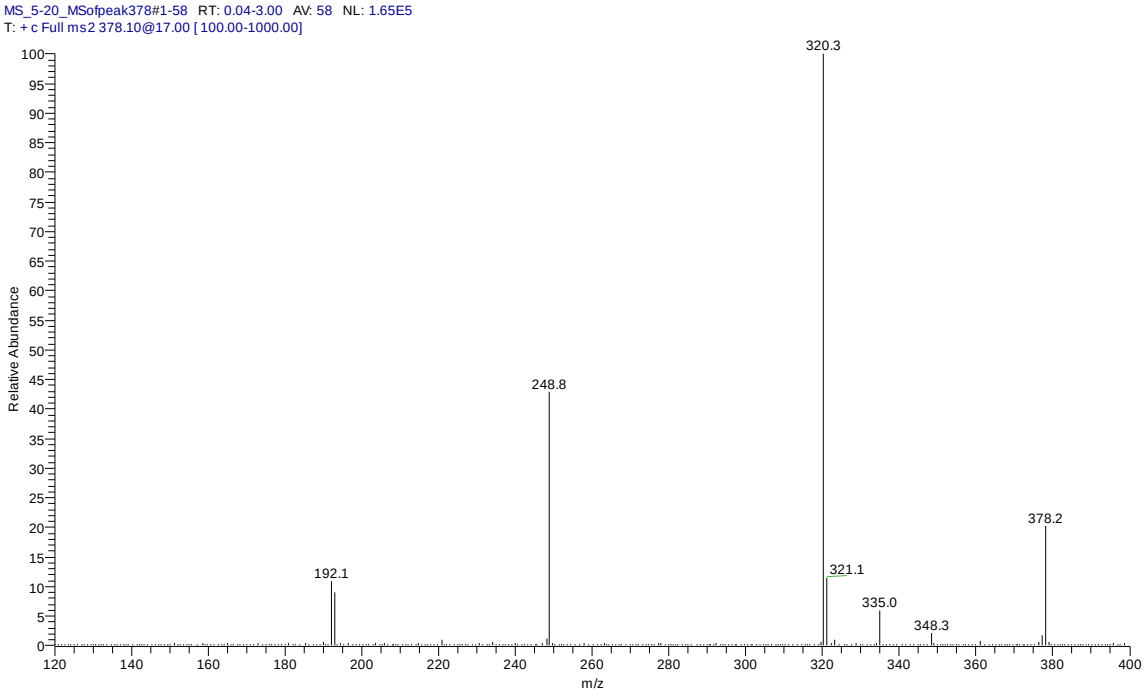

Figure 4. 11 Fragmentation of Cu-PPI complex at m/z = 378.2.

of the neutral loss of 58, for instance, the N-C dendrimer bond between one interior nitrogen and the carbon of the propyl amine undergoes homolytic cleavage resulting in a $NH_2CH_2CH_2CH_2\cdot$ leaving group (mass is neutral 58) and the dendrimer with the interior nitrogen as a radical.

The neutral loss of 129 occurs through a proton transfer similar to the neutral loss of 131 in the other metal species, however, in the case of this complex, the proton transfer is not to the leaving group, but to the group that retains the metal. The subsequent loss from this ion at m/z = 249 is neutral loss of 57. This loss, although a similar mass to losses seen in the other metal

species, is not a propyl amine group, but the butane core fragmenting through a radical mechanism. This identification is confirmed with the ^{15}N labeled dendrimer where this loss is still 57 and not 58 as it would be if it were a propyl amine group. It is also interesting to note that the ion at m/z = 163 picks up a neutral adduct upon isolation and storage, but as opposed to the water like the Zn and Co complexes, the adduct is acetonitrile.

The full fragmentation scheme is shown in Figure 4.12.

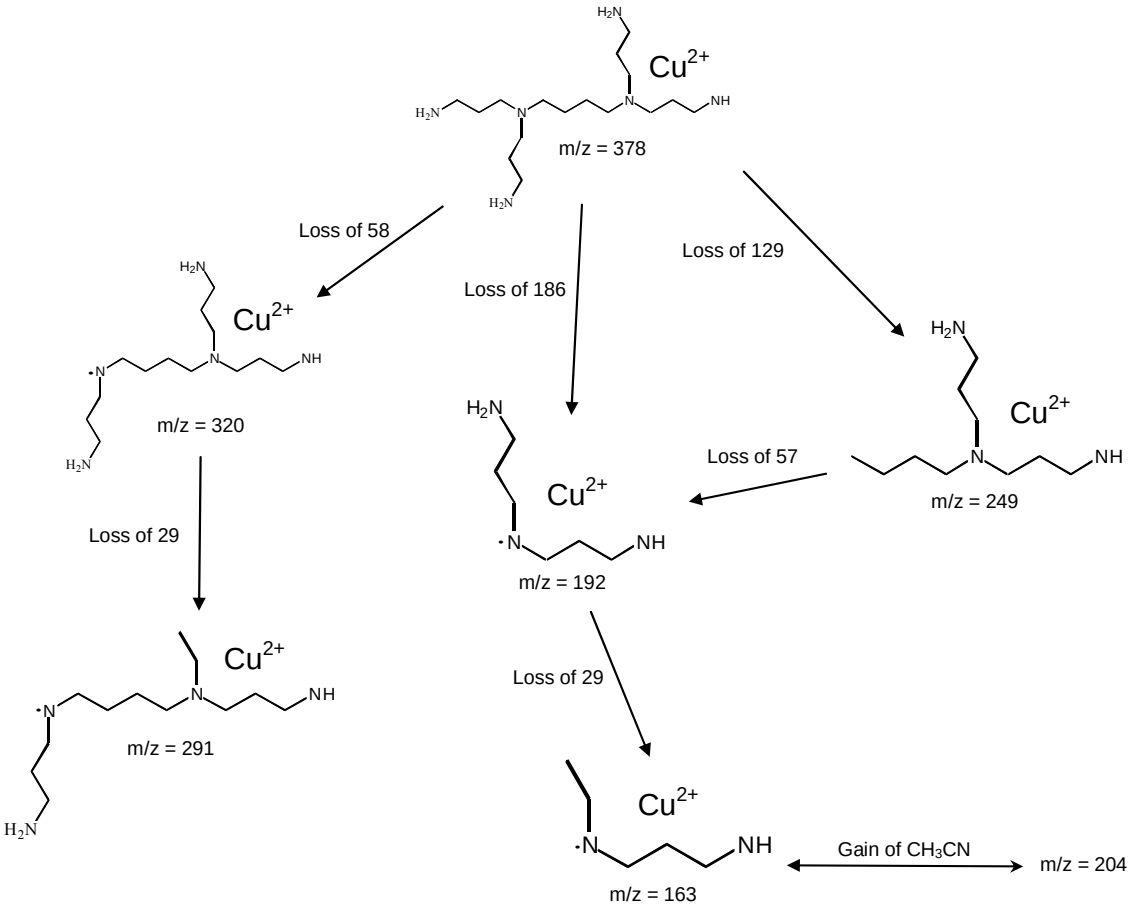

Figure 4. 12 Fragmentation scheme of Cu-PPI complex showing neutral losses and resulting charged fragments.

DISCUSSION

Now that the protonated dendrimer and all four metal complexes have been presented, comparisons can be made between fragmentations and mechanisms. A primary neutral loss table is shown in Table 4.2. Primary neutral losses come from exterior branches of the dendrimer or

Table 4. 2 Primary neutral loss table for PPI dendrimer complexes. Compare similar primary losses from cobalt, nickel and zinc with markedly different losses for copper.

Formula	Fragment	Mass	H+	Co	Ni	Cu	Zn
	H_2	2	-	2,3	2,3,4	3	2,3,4
	NH_3	17	4	2,3	2,3,4	-	2,3
CH_3N	$HN{=}CH_2$	29	-	-	2,3	3	2,3
CH_5N	NH_2CH_3	31	-	4	-	-	-
C_2H_5N	$NH_2CH{=}CH_2$	43	-	-	2,3	2,3	3
C_3H_7N		57	3,4	2,3	2,3,4	-	2,3
C_3H_8N	$NH_2(CH_2)_2CH_2\bullet$	58	-	-	-	2	-
$C_6H_{15}N_3$	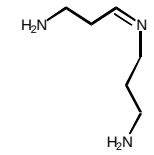	129	-	-	-	2	-
$C_6H_{17}N_3$	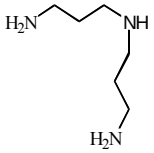	131	2	2	-	-	2
$C_{10}H_{23}N_3$	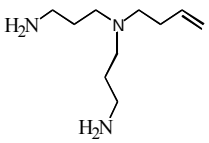	185	-	2	2	-	2
$C_{10}H_{24}N_3$	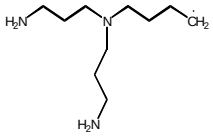	186	-	-	-	2	-

larger fragments. These losses can occur in multiple stages of fragmentation. The number refers to the generation of mass spectrometry (MS) in which the fragment was identified. With the exception of the Copper-PPI complex that fragments through a proposed radical mechanism, the Cobalt, Nickel and Zinc-PPI complexes have similar primary neutral losses. There is no structure given for the fragment at 57 because two different structures are proposed; one for the protonated and a different one for the metal complexes.

A secondary neutral loss table is shown in Table 4.3. Secondary neutral losses come from fragments that have already lost at least one primary fragment. The number refers to the generation of MS in which the fragment was identified. These secondary losses demonstrate metal specificity, meaning some losses are unique to each metal complex.

Of particular interest is the neutral loss of 55 that occurs in the Nickel and Zinc complexes. This loss of 55 has been identified only from a dendrimer species that had previously lost a neutral NH_3. As evidenced by the ^{15}N labeled fragmentation, this fragment contains an exterior nitrogen. It appears that this loss of 55 occurs in two steps: step one involves a proton transfer to the interior tertiary amine and formation of a double bond on the leaving group and step two is a H_2 transfer from the N-C bond of the leaving group to the C=C bond that has previously lost the ammonia. As previously mentioned this loss only occurs in the Nickel and Zinc complexes. This specificity implicates a higher order geometry possibly dependant on the spin state and/or coordination of the complex.

Table 4. 3 Secondary neutral loss table for PPI dendrimer complexes. Note the metal specificity in secondary losses.

Formula	Fragment	Mass	H+	Co	Ni	Cu	Zn
C_2H_4	$CH_2=CH_2$	28	5	-	-	-	-
C_3H_6	$CH_3CH=CH_2$	42	5	5	3	-	-
C_4H_6	$CH_2=CHCH=CH_2$	54	-	-	-	-	3
C_3H_5N	$NH=CHCH=CH_2$	55	-	-	3	-	3
C_4H_8	$CH_2=CHCH_2CH_3$	56	-	3	-	-	-
C_4H_9	$CH_3(CH_2)_2CH_2\bullet$	57	-	-	-	3	-
C_4H_9N	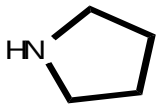	71	4	-	-	-	-
$C_3H_{10}N_2$	$NH_2(CH_2)_3NH_2$	74	-	3	3,4	-	3
$C_4H_{12}N_2$		88	-	3	-	-	-
$C_5H_{14}N_2$		102	-	-	-	-	3
$C_7H_{16}N_2$		128	3	3	-	-	3
$C_9H_{20}N_2$	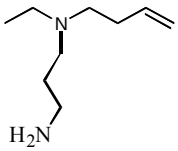	156	-	-	-	-	3
$C_{10}H_{20}N_2$	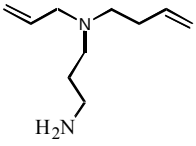	168	-	3	-	-	-

CHAPTER FIVE: CONCLUSIONS

Mass spectrometry has been shown to be a sensitive method to elucidate the gas-phase composition of complexes involving a 1st generation PPI dendrimers and divalent metals. Comparisons between monoisotopic and isotopically labeled dendrimers have allowed unambiguous identification of neutral losses and provided evidence for fragmentation mechanisms. Variability in the fragmentation with adducted transition metal, that becomes more metal specific as the fragmentation generation increases, suggests some higher order geometry possibly dependant on spin state and/or coordination of the complex. Several complexes pick up neutral adducts upon isolation and storage in the ion-trap presumably due to a thermodynamic need to complete the coordination shell. Dehydrogenation is a dissociation pathway in all complexes.

APPENDIX

This appendix contains representative raw mass spectra for the monoisotopic protonated and metal complexed dendrimers.

Protonated PPI – Fragmentation of m/z = 317

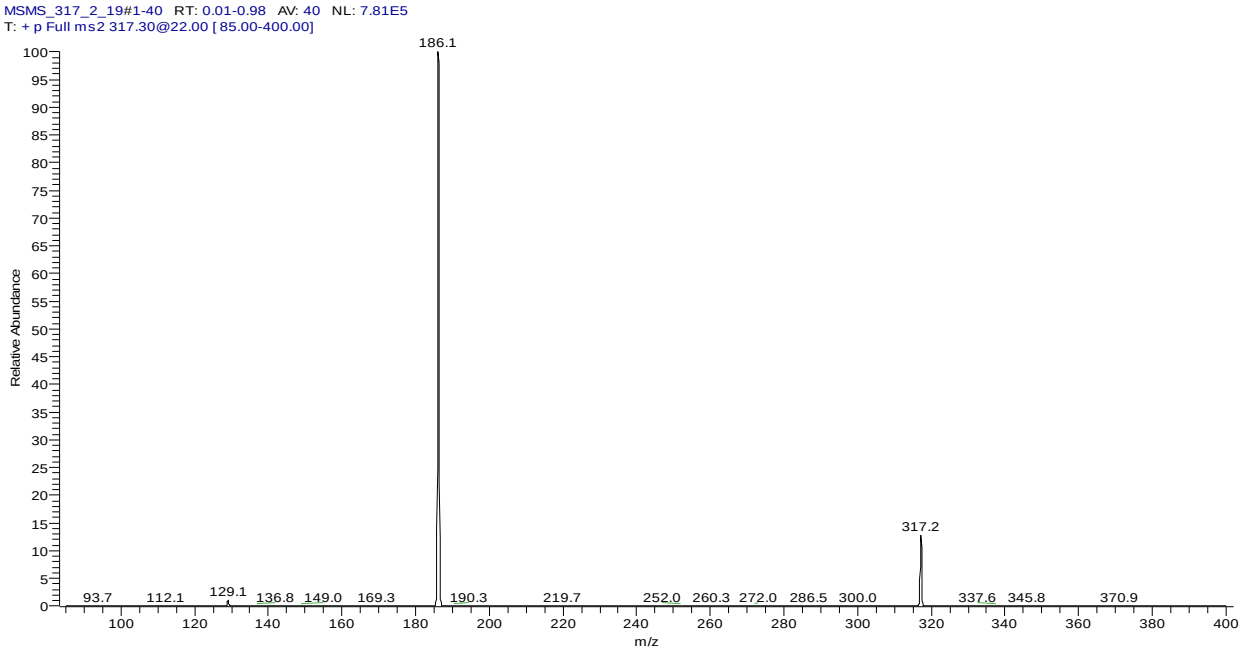

Protonated PPI – Fragmentation of m/z = 186

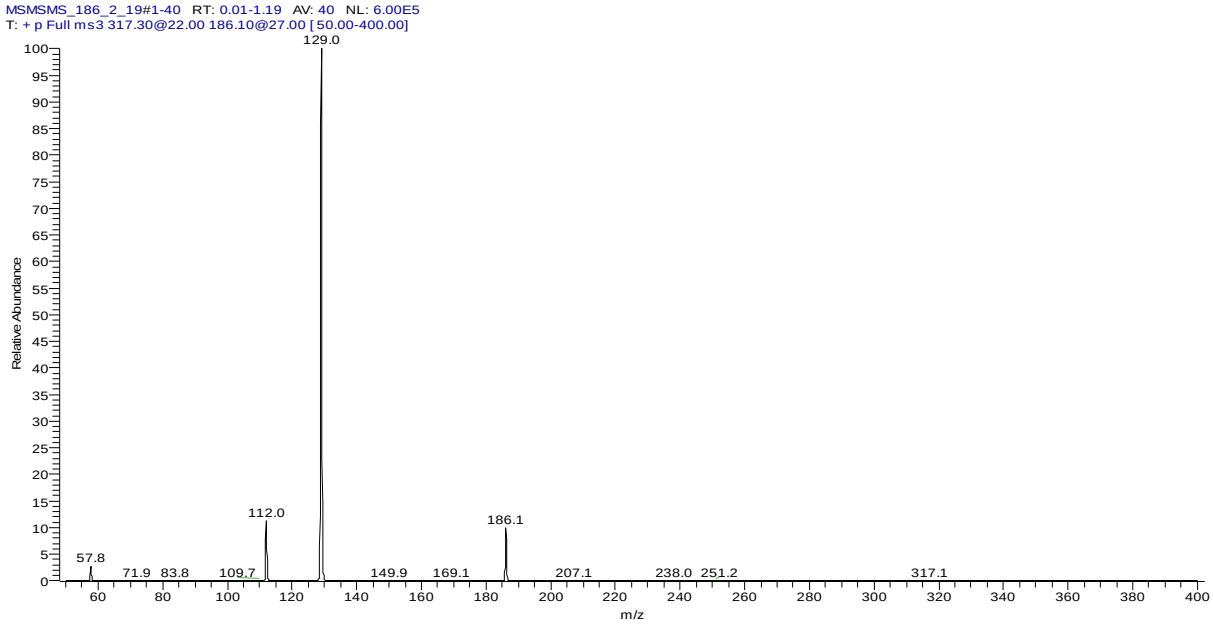

Protonated PPI – Fragmentation of m/z = 129

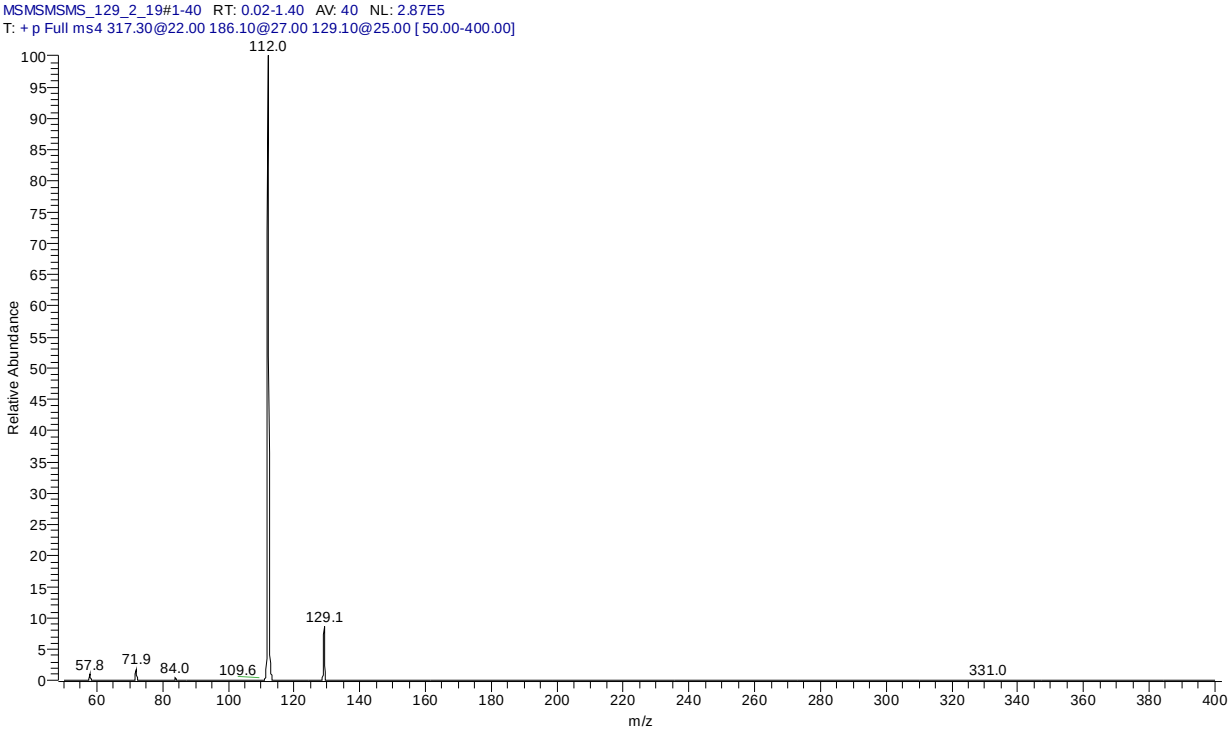

Protonated PPI – Fragmentation of m/z = 112

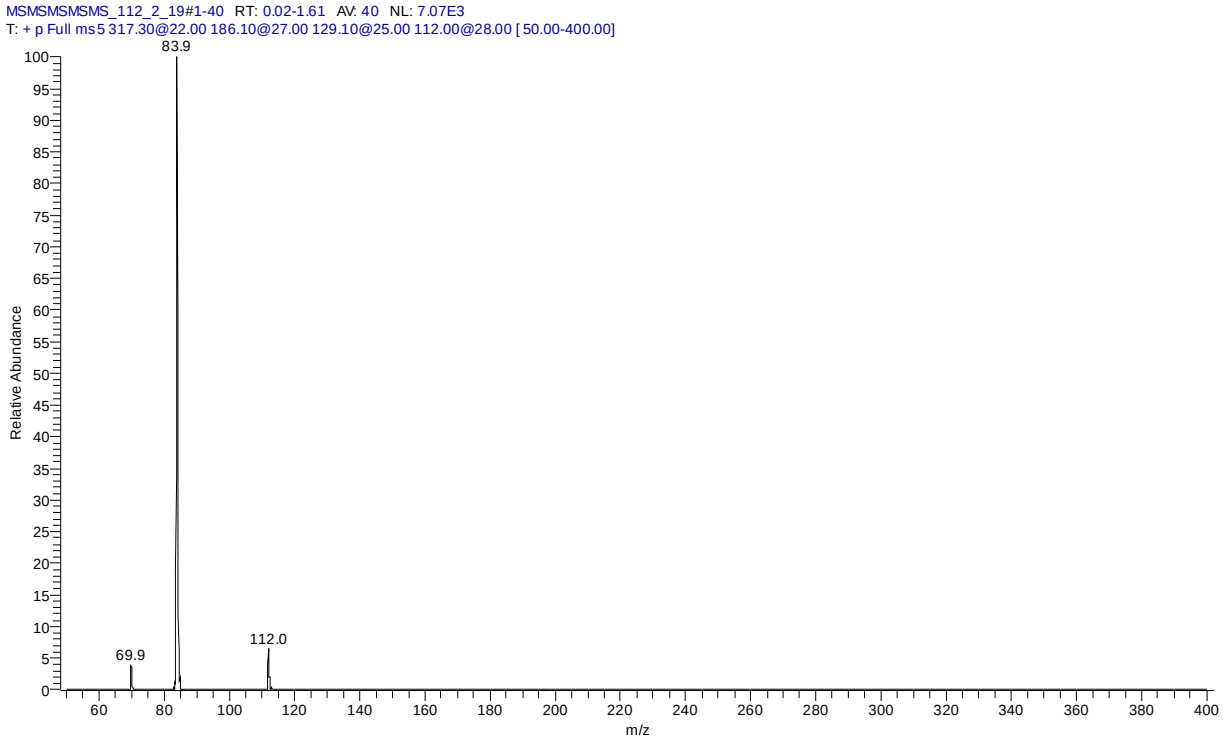

Cobalt PPI – Fragmentation of m/z = 374

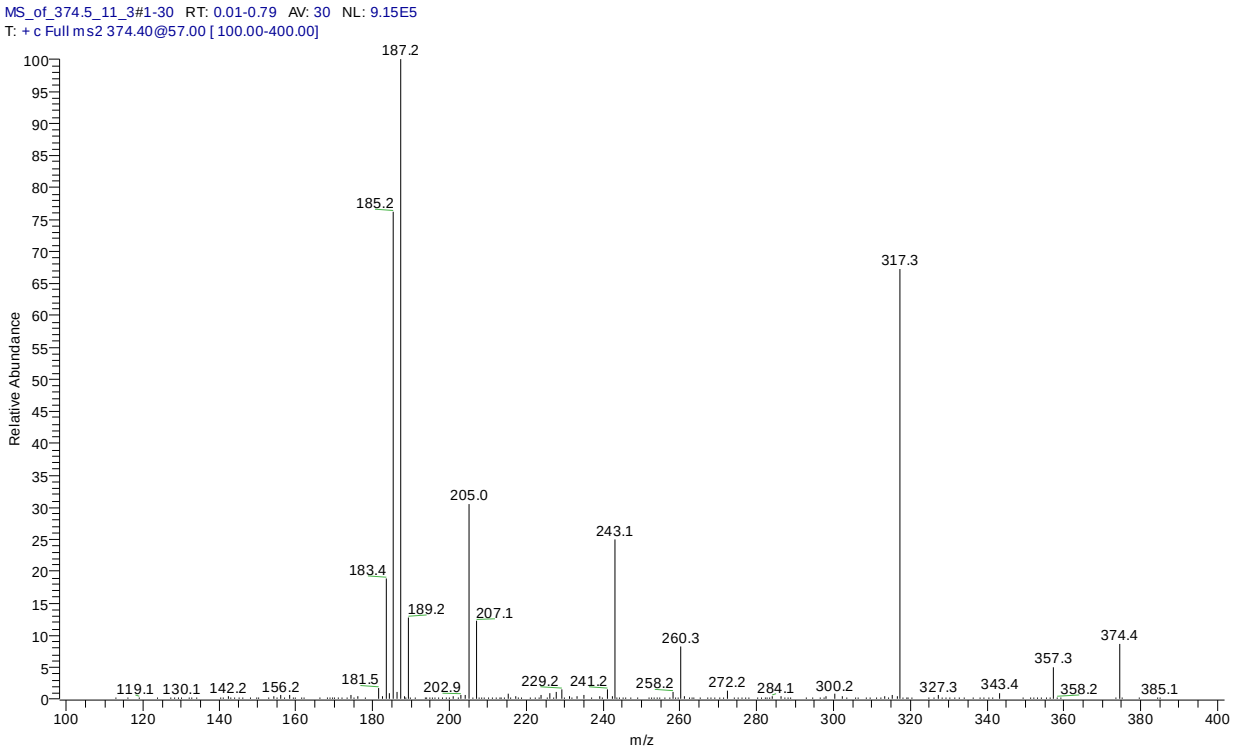

Cobalt PPI – Fragmentation of m/z = 357

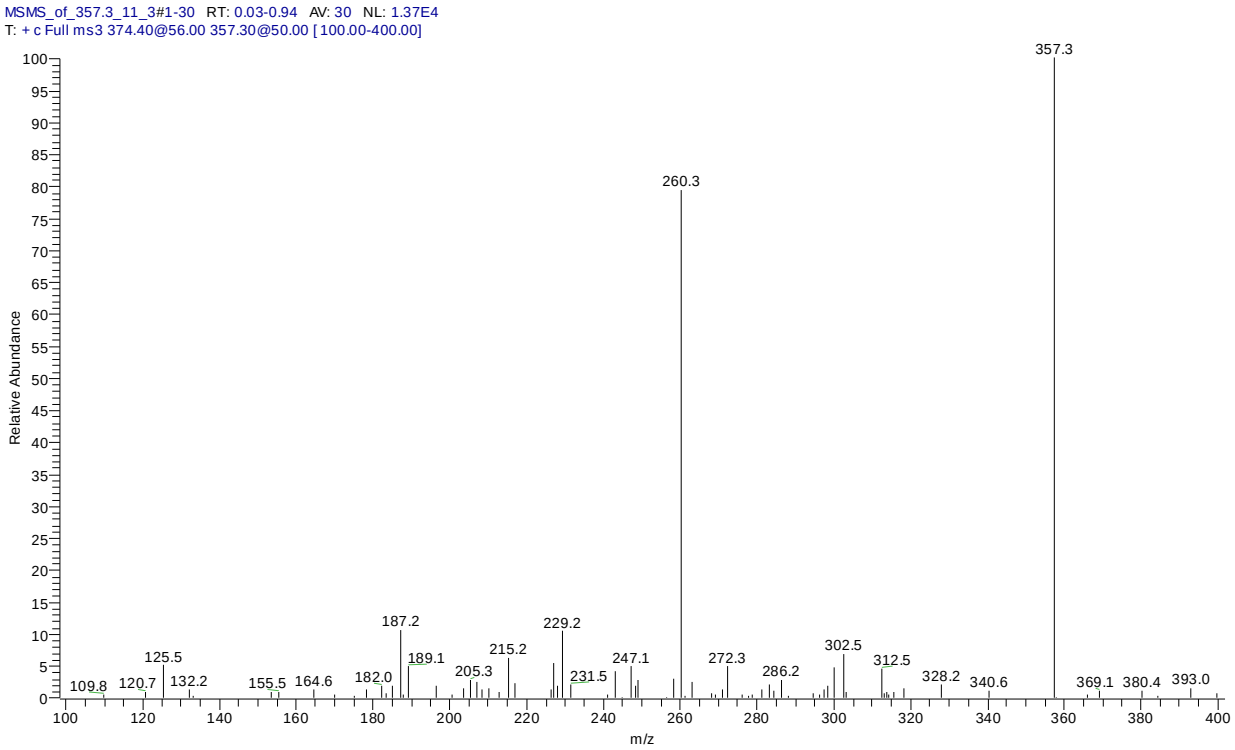

Cobalt PPI – Fragmentation of m/z = 317

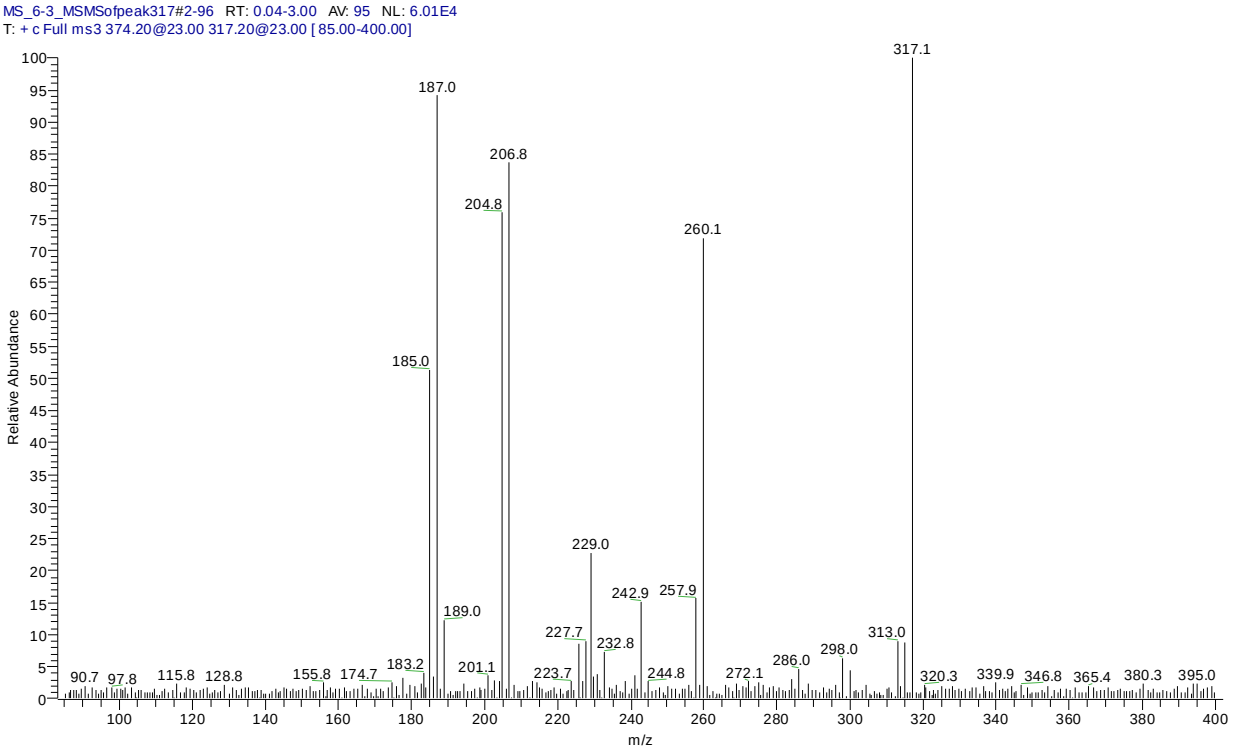

Cobalt PPI – Fragmentation of m/z = 260

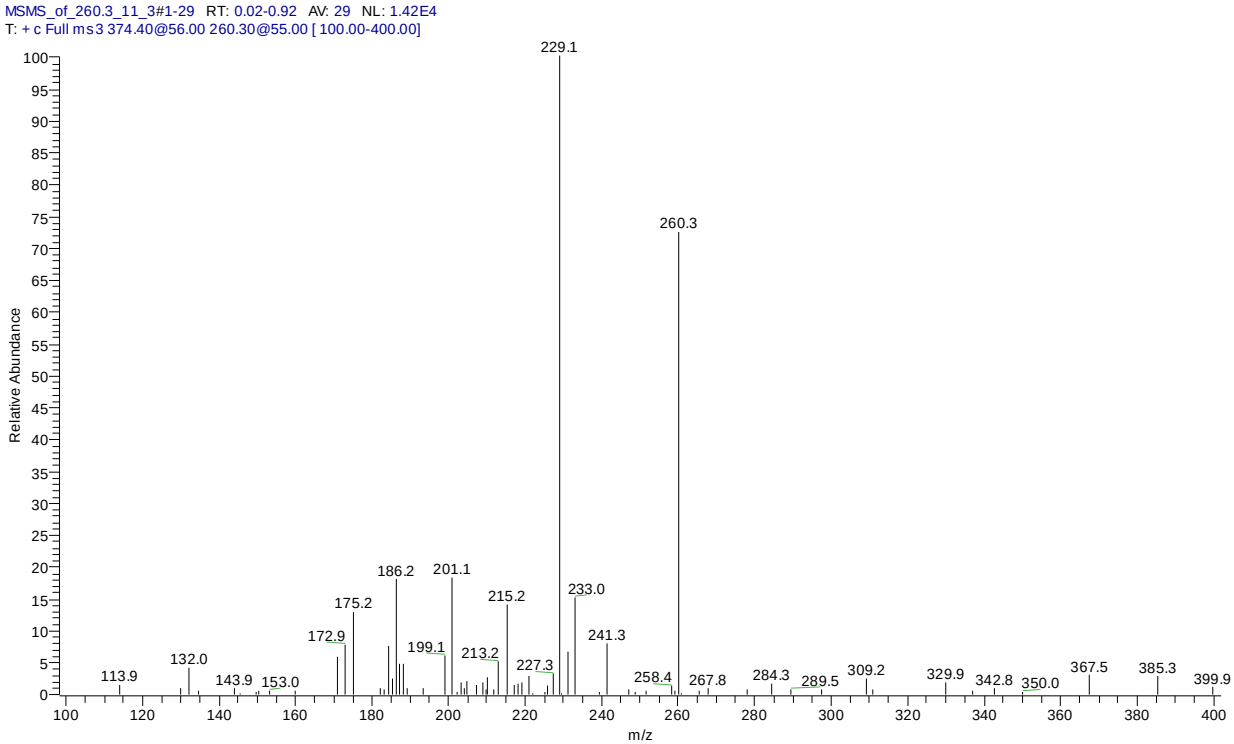

Cobalt PPI – Fragmentation of m/z = 242

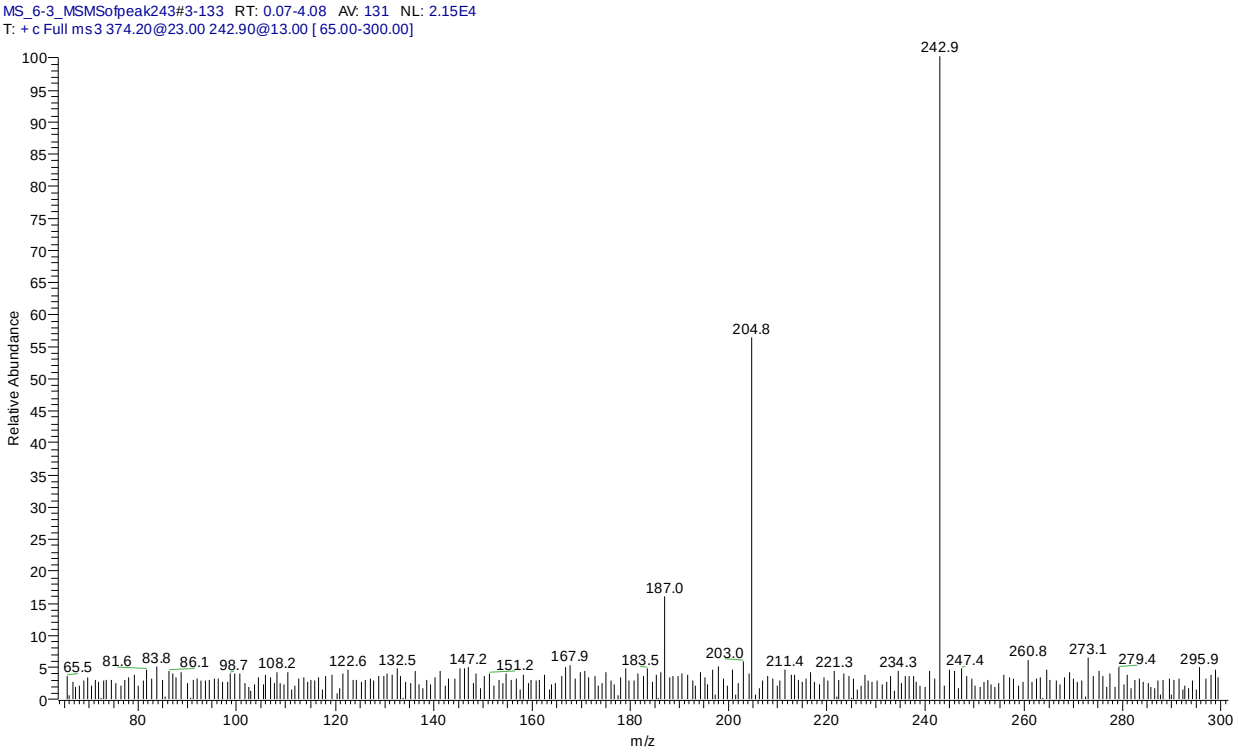

Cobalt PPI – Fragmentation of m/z = 205

Nickel PPI – Fragmentation of m/z = 373

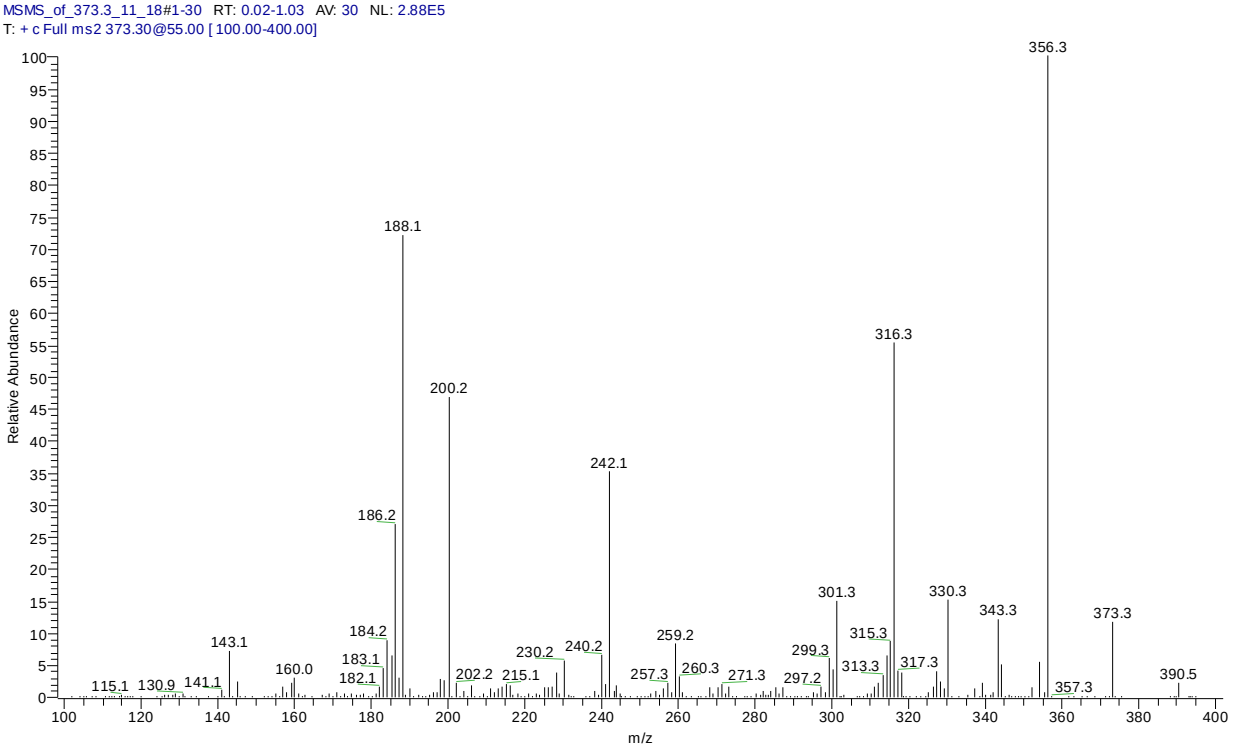

Nickel PPI – Fragmentation of m/z = 356

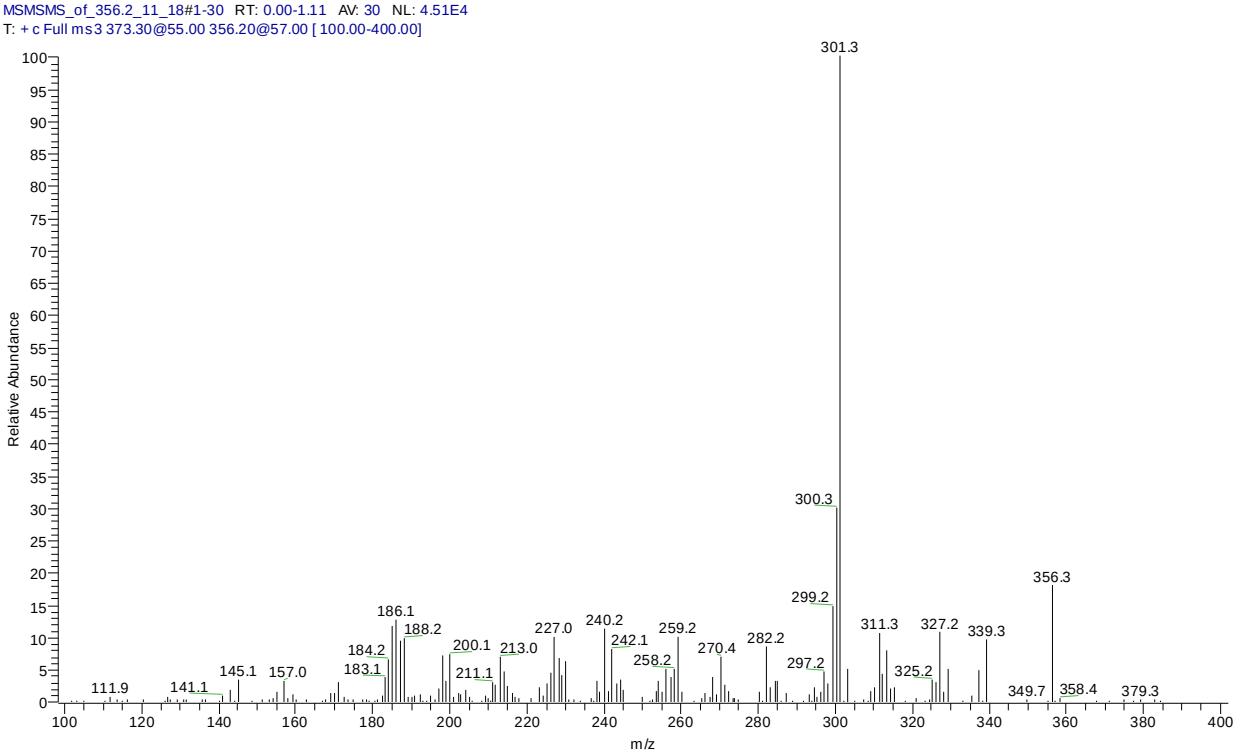

Nickel PPI – Fragmentation of m/z = 316

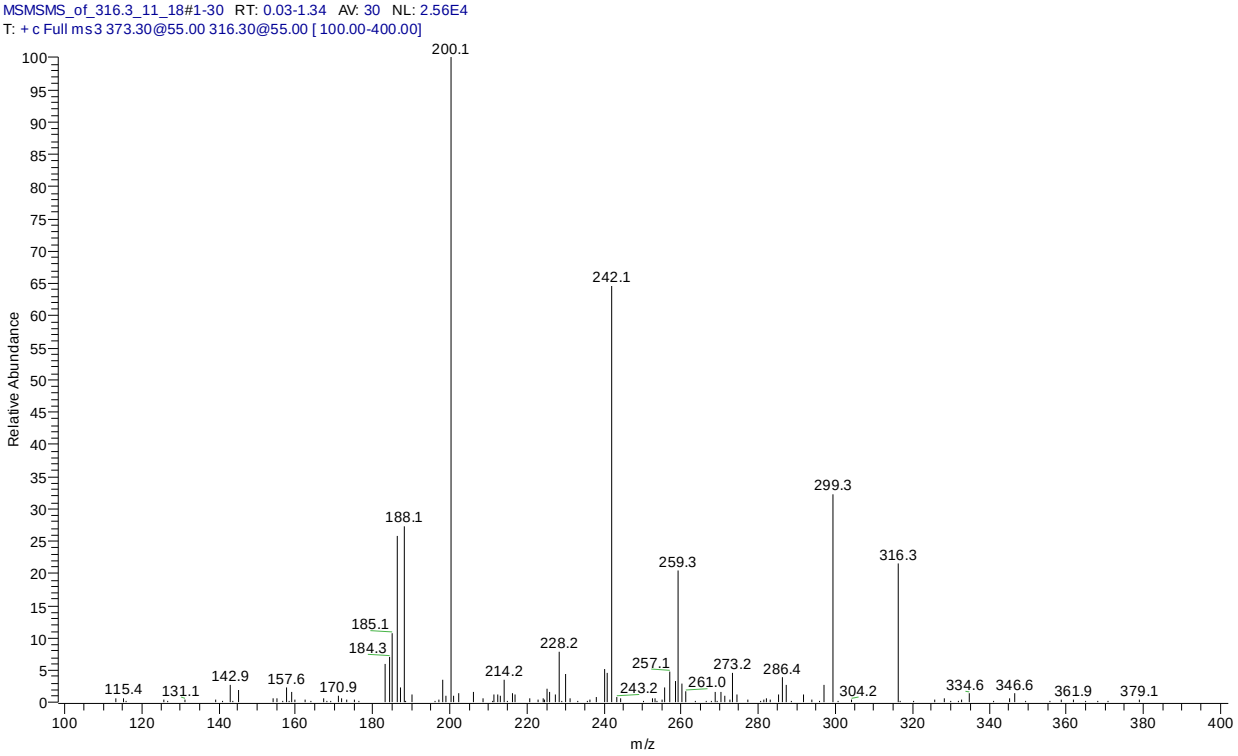

Nickel PPI – Fragmentation of m/z = 242

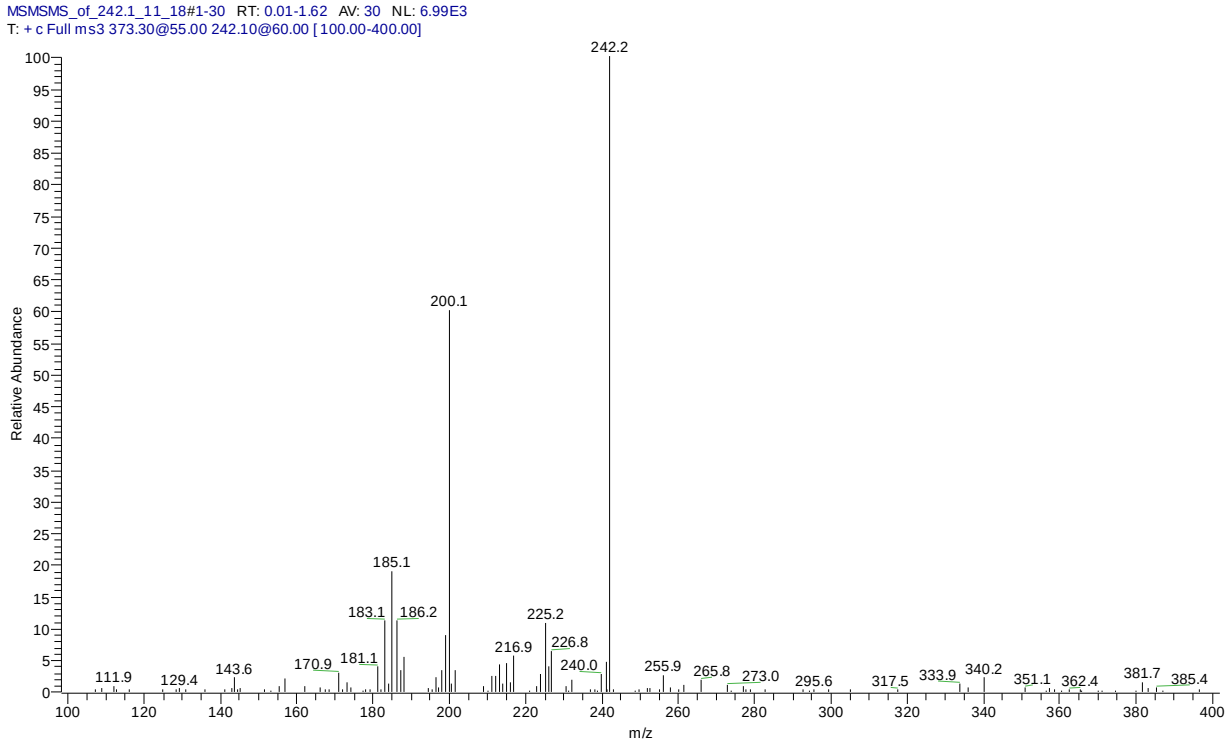

Nickel PPI – Fragmentation of m/z = 200

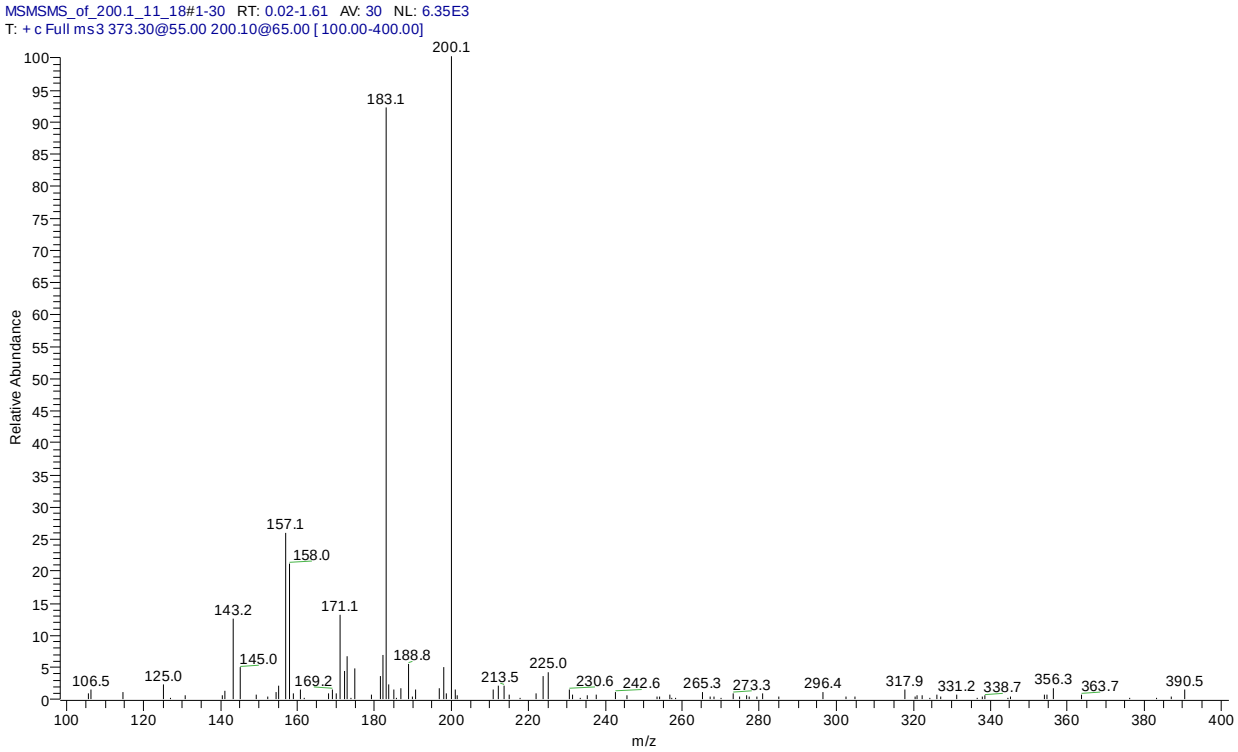

Nickel PPI – Fragmentation of m/z = 188

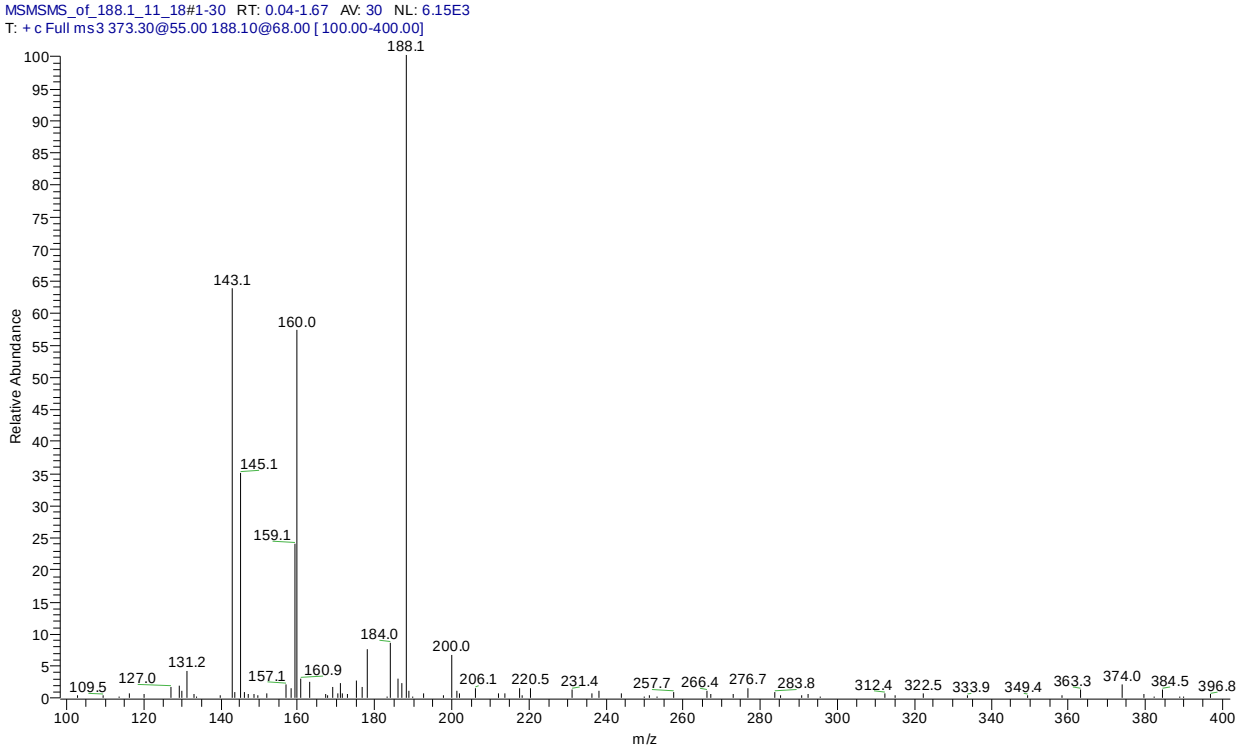

Copper PPI – Fragmentation of m/z = 378

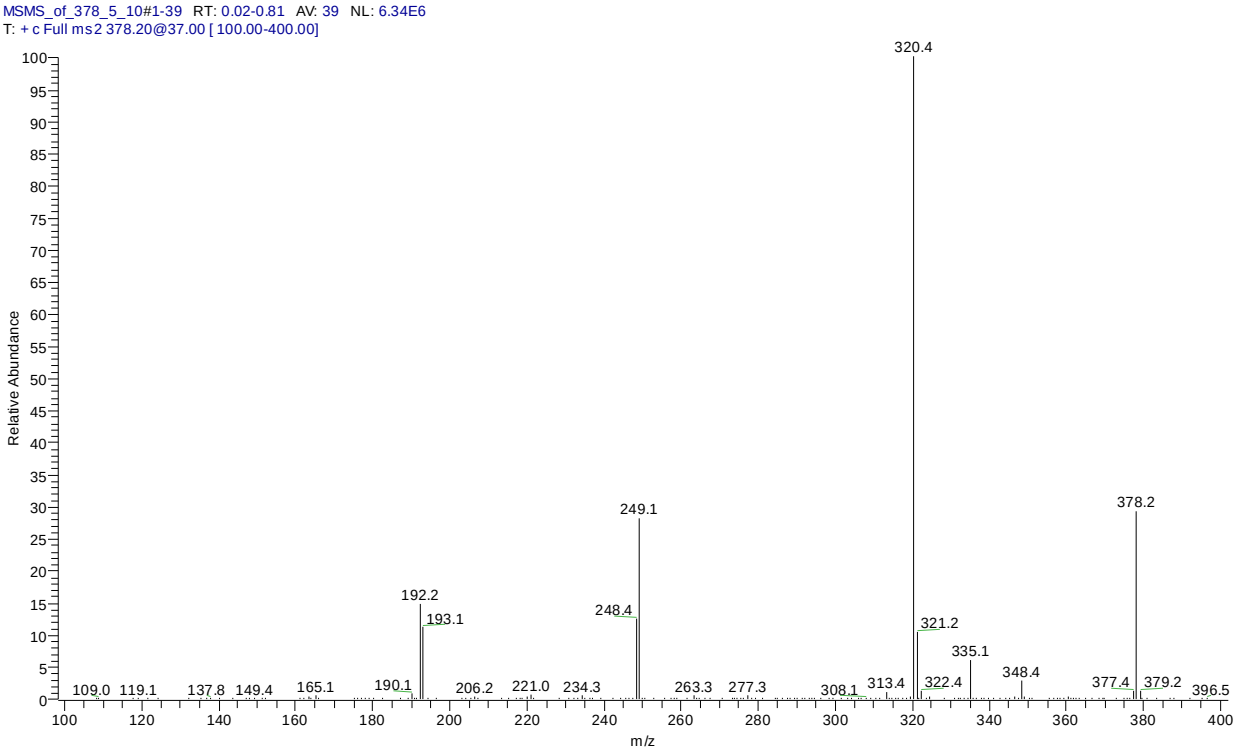

Copper PPI – Fragmentation of m/z = 320

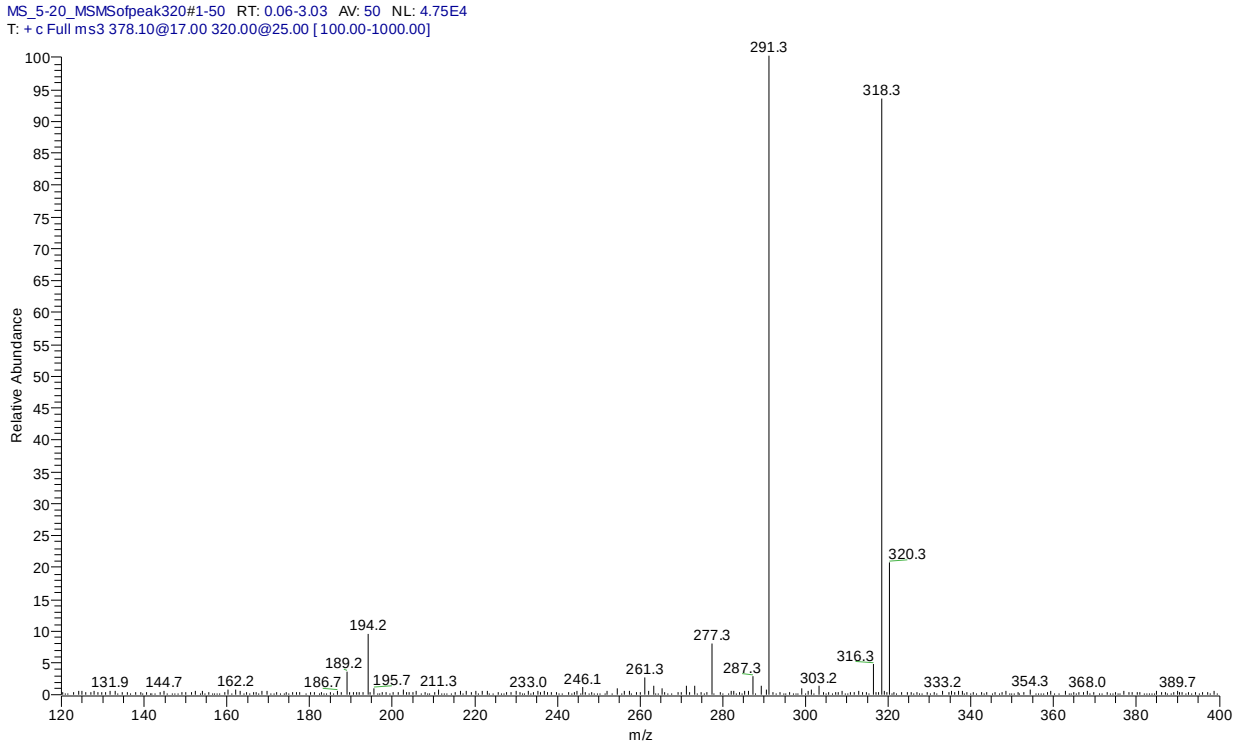

Copper PPI – Fragmentation of m/z = 248

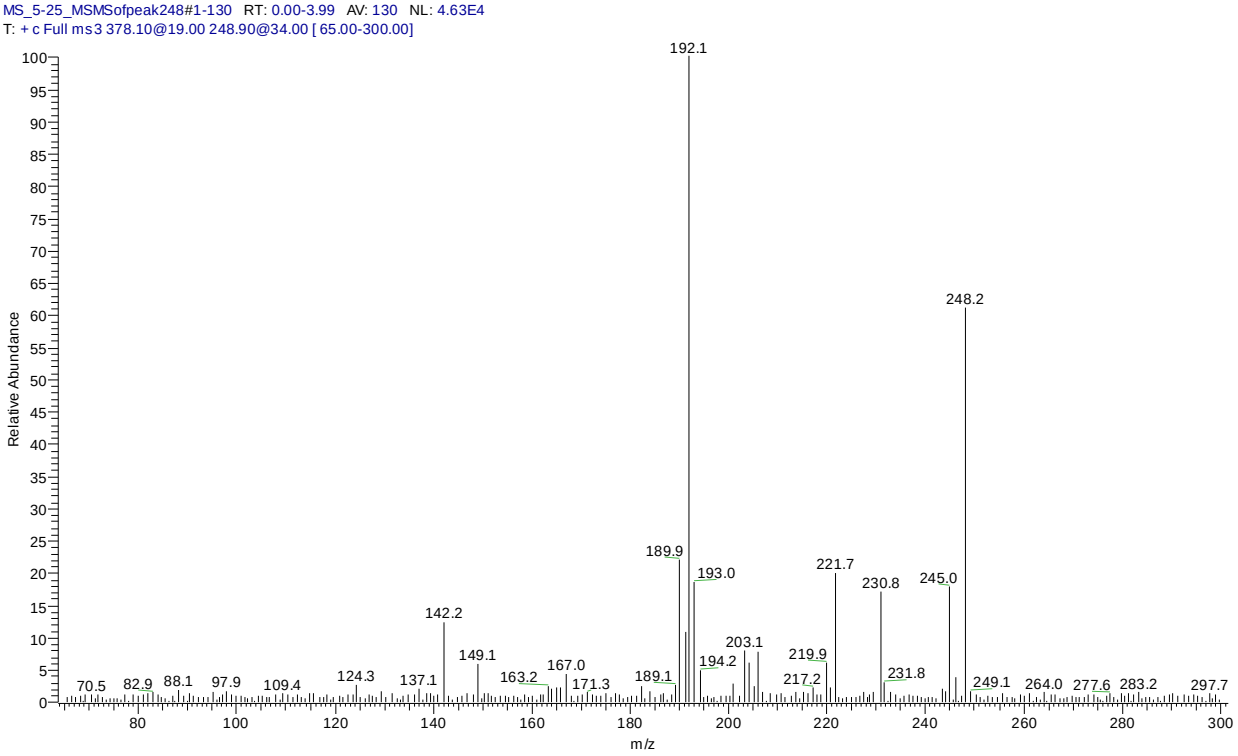

Copper PPI – Fragmentation of m/z = 192

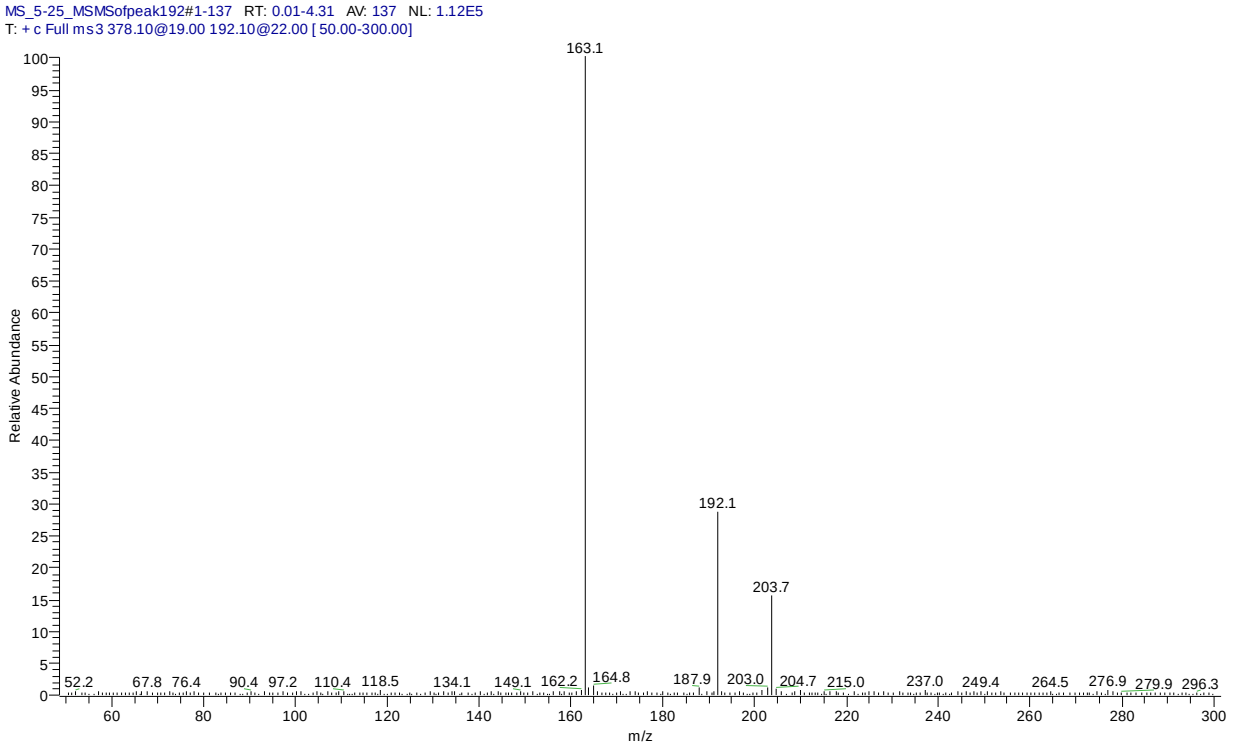

Zinc PPI – Fragmentation of m/z = 379

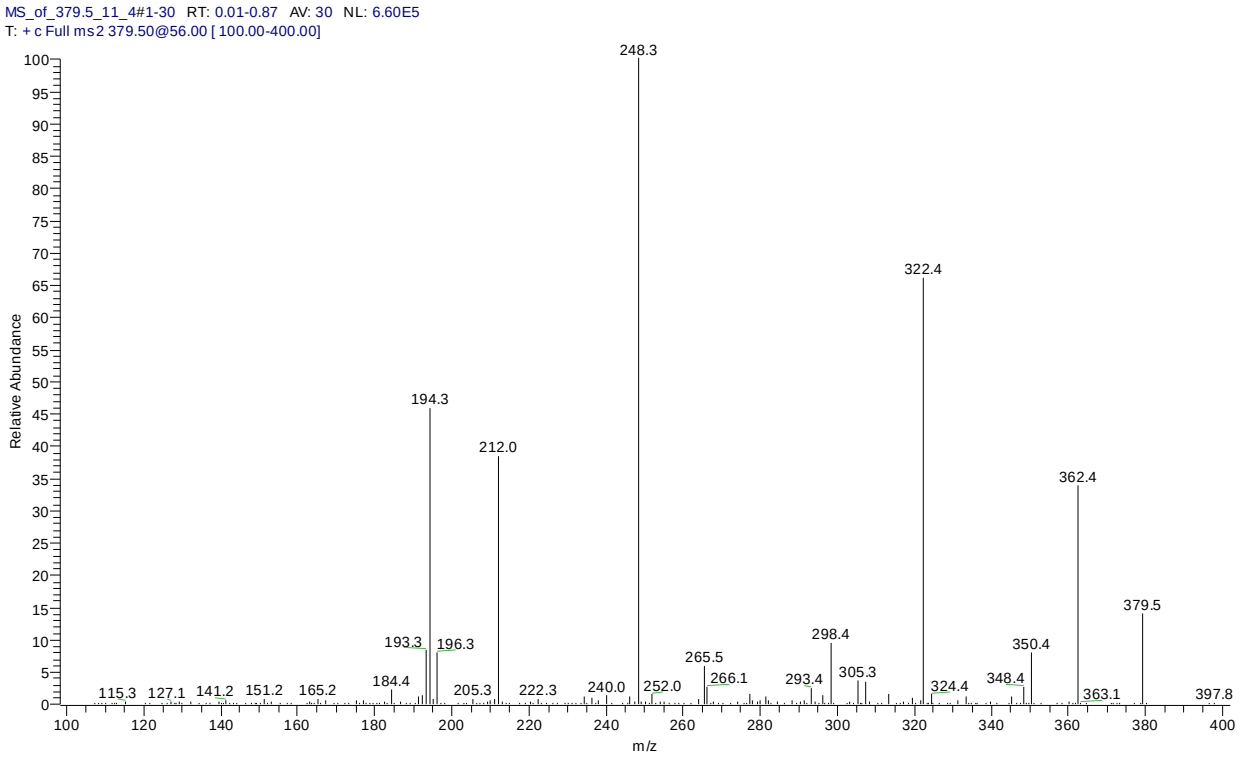

Zinc PPI – Fragmentation of m/z = 362

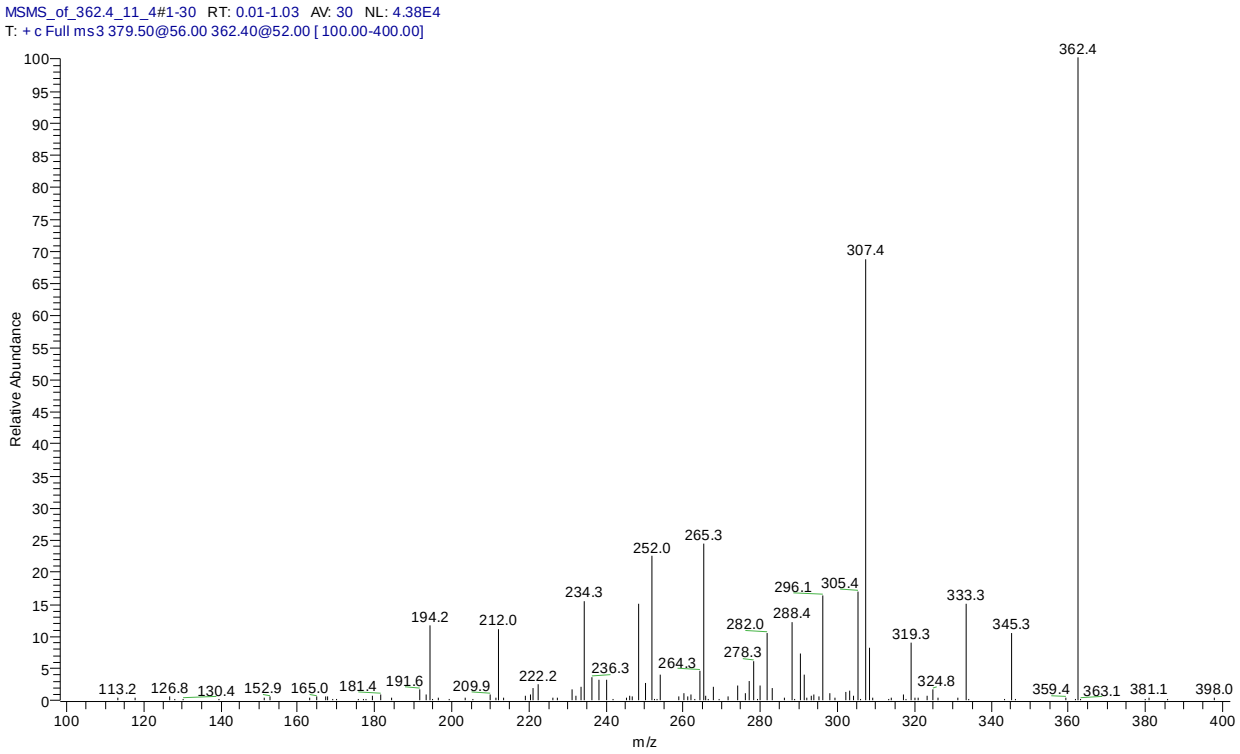

Zinc PPI – Fragmentation of m/z = 350

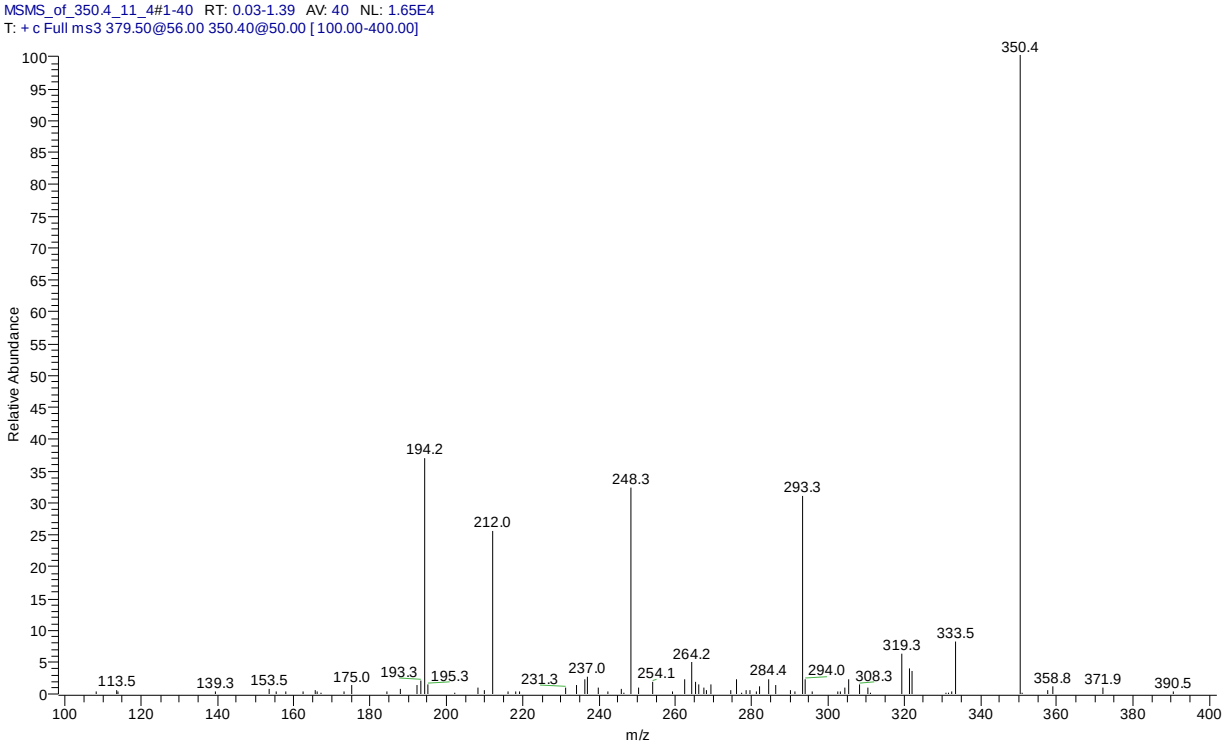

Zinc PPI – Fragmentation of m/z = 307

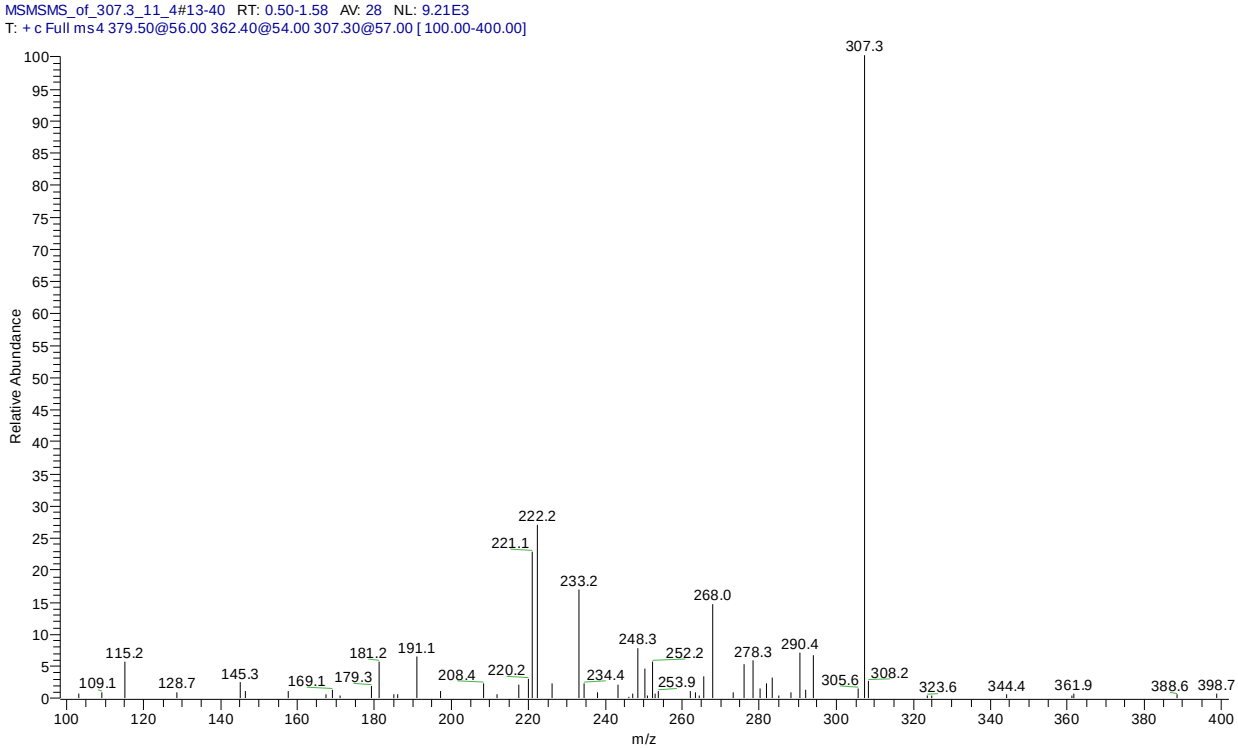

Zinc PPI – Fragmentation of m/z = 248

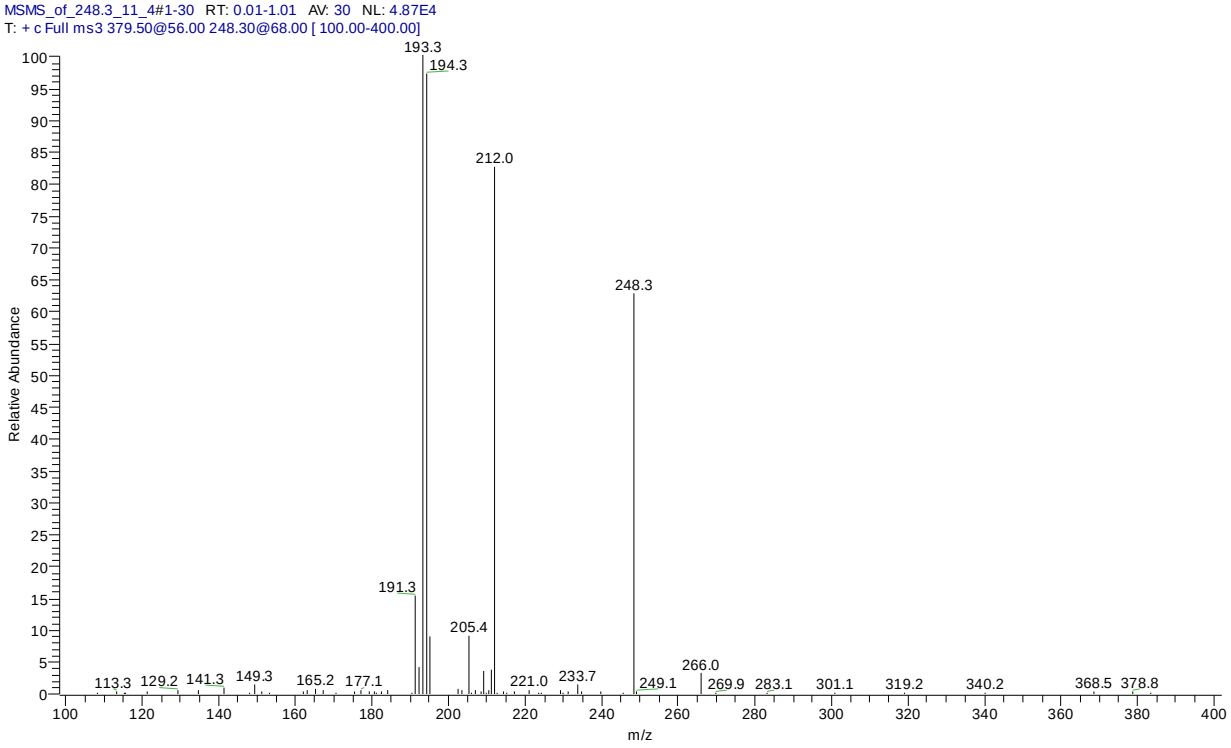

Zinc PPI – Fragmentation of m/z = 194

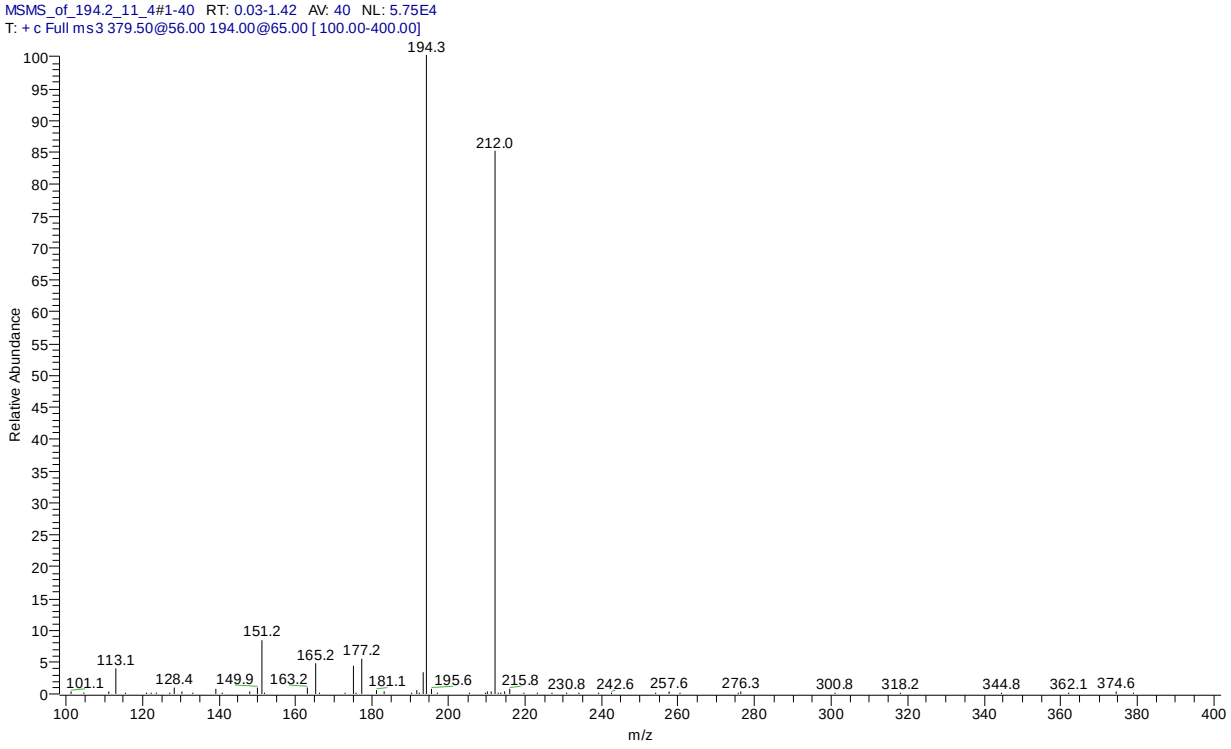

REFERENCES

1. Tomalia, D.A.; Naylor, A.M.; Goddard III, W.A. *Angew. Chem. Int. Ed. Engl.* **1990**, 29, 138.
2. Buhleier, E.; Wehner, W.; Vögtle, F. *Synth. Commun.* **1978**, 2, 155.
3. Wörner, C.; Mülhaupt, R. *Angew. Chem. Int. Ed. Engl.* **1993**, 32, 1306.
4. de Brabander-van den Berg, E.M.M.; Meijer, E.W. *Angew. Chem. Int. Ed. Engl.* **1993**, 32, 1308.
5. Tomalia, D.A.; Hall, M.; Hedstrand, D.M. *J. Am. Chem. Soc.* **1987**, 109, 1601.
6. Stoddart, F.J.; Welton, T. *Polyhedron* **1999**, 18, 3575.
7. Newkome, G.R.; Yao, Z-q.; Baker, G.R.; Gupta, V.K.; Russo, P.S.; Saunders, M.J. *J. Am. Chem. Soc.* **1986**, 108, 849.
8. Hawker, C.J.; Fréchet, J.M.J. *J. Am. Chem. Soc.* **1990**, 112, 7638.
9. Hodge, P. *Nature* **1993**, 362, 18.
10. Service, R.F. *Science* **1995**, 267, 458.
11. Alper, J. *Science* **1991**, 251, 1562.
12. Fréchet, J.M.J. *Science* **1994**, 263, 1710.
13. Tomalia, D.A.; Dvornic, P.R. *Nature* **1994**, 372, 617.
14. Reetz, M.T.; Lohmer, G.; Schwickardi, R. *Angew. Chem. Int. Ed. Engl.* **1997**, 36, 1526.
15. Crooks, R.M.; Zhao, M.; Sun, L.; Chechik, V.; Yeung, L.K. *Acc. Chem. Res.* **2001**, 34, 181.
16. Scott, R.W.J.; Wilson, O.M.; Crooks, R.M. *J. Phys. Chem. B* **2005**, 109, 692.
17. Stevelmans, S.; van Hest, J.C.M.; Jansen, J.F.G.A.; van Boxtel, D.A.F.J.; de Brabander-van den Berg, E.M.M.; Meijer, E.W. *J. Am. Chem. Soc.* **1996**, 118, 7398.
18. Issberner, J.; Moors, R.; Vögtle, F. *Angew. Chem. Int. Ed. Engl.* **1994**, 33, 2413.
19. Zanini, D.; Roy, R. *J. Am. Chem. Soc.* **1997**, 119, 2088.
20. Halford, B. "Dendrimers Branch Out" Chemical and Engineering News June 13, 2005, 30.
21. Mcluckey, S.A.; Asano, K.G.; Schaaff, T.G.; Stephenson, J.L. Jr. *Int. J. Mass Spectrom.* **2000**, *195/196*, 419.
22. Bouchoux, G.; Choret, N.; Berruyer-Penaud, F.; Flammang, R. *Int. J. Mass Spectrom.* **2002**, *217*, 195.